Secondary Nucleation in Amyloid Formation

Törnquist, Mattias

2020

Document Version:
Publisher's PDF, also known as Version of record

Secondary nucleation in amyloid aggregation

MATTIAS TÖRNQUIST | BIOCHEMISTRY AND STRUCTURAL BIOLOGY | LUND UNIVERSITY

$$\frac{dP}{dT} = k_n \frac{m(t)^{n_c}}{1 + \left(\frac{m(t)}{K_P}\right)^{n_c}} + k_2 \frac{m(t)^{n_2}}{1 + \left(\frac{m(t)}{K_S}\right)^{n_2}} M(t)$$

$$\frac{dM}{dT} = 2k_+ \frac{m(t)}{1 + \frac{m(t)}{K_E}} P(t)$$

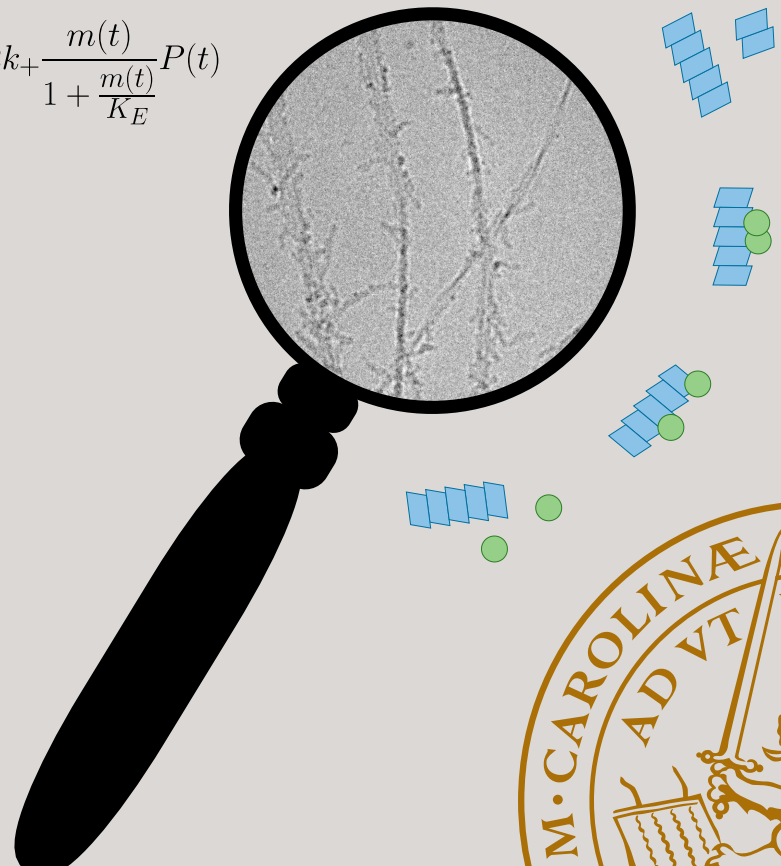

Secondary nucleation in amyloid formation

Secondary nucleation in amyloid formation

by Mattias Törnquist

LUND
UNIVERSITY

Thesis for the degree of Doctor of Philosophy

Thesis advisors: Prof. Sara Linse,
Assoc. Prof. Tommy Cedervall, Thom Leiding

Faculty opponent: Prof. David Eisenberg, UCLA, USA

To be presented, with the permission of the Faculty of Science of Lund University, for public criticism in the K:A lecture hall at the Department of Chemistry on Thursday, the 4th of June 2020 at 15:00.

Organization
LUND UNIVERSITY

Department of Chemistry
Box 118
SE–221 00 LUND
Sweden

Document name
DOCTORAL DISSERTATION

Date of disputation
2020-06-04

Sponsoring organization

Author(s)
Mattias Törnquist

Title and subtitle
Secondary nucleation in amyloid formation:

Abstract
Research into Alzheimer's disease is still hampered by a lack of fundamental understanding of the underlying mechanisms. While the aggregation of the amyloid β peptide into amyloid fibrils is highly implicated as a key factor in the disease, the molecular nature of its involvement has proven complex and elusive. This thesis and the work herein is part of an ongoing effort to map out the aggregation mechanism of $A\beta$ *in vitro* in as much detail as possible, in the hope to provide a better basis for understanding its role in disease. In particular, the mechanism of secondary nucleation, whereby the fibril surface catalyses the formation of new fibrils is of interest due to its capacity to generate large numbers of toxic oligomers. In this work, we probe the determinants of secondary nucleation by studying its influence in different temperatures and pH and we confirm that it remains an important factor in aggregation in human cerebrospinal fluid. We also report a transient accumulation of pre-fibrillar aggregates, likely to be a result of heavily saturated secondary nucleation, which can form a basis for further structural studies of this phenomenon.

Key words
Alzheimer's disease, amyloid, $A\beta 42$, aggregation mechanism, aggregation kinetics, secondary nucleation, protein misfolding

Classification system and/or index terms (if any)

Supplementary bibliographical information

Language
English

ISSN and key title

ISBN
978-91-7422-740-6 (print)
978-91-7422-747-5 (pdf)

Recipient's notes

Number of pages
64

Price

Security classification

Secondary nucleation in amyloid formation

by Mattias Törnquist

LUND
UNIVERSITY

Cover illustration front: Picture by the author. *cryo*-EM image of large prefibrillar oligomers growing on a the surface of fibrils.

Cover illustration back: Picture by the author. I do not apologize.

Faculty of Science, Department of Chemistry

ISBN: 978-91-7422-740-6 (print)
ISBN: 978-91-7422-747-5 (pdf)

Printed in Sweden by Media-Tryck, Lund University, Lund 2020

Media-Tryck is a Nordic Swan Ecolabel certified provider of printed material. Read more about our environmental work at www.mediatryck.lu.se

MADE IN SWEDEN

"Your own brain ought to have the decency to be on your side"
sir Terry Pratchett, Wintersmith

Contents

List of publications

This thesis is based on the following publications, referred to by their Roman numerals:

I **Autocatalytic amplification of Alzheimer associated Aβ42 peptide aggregation in human cerebrospinal fluid**
R. Frankel and M. Törnquist, G. Meisl, O. Hansson, U. Andreasson, H. Zetterberg, K. Blennow, B. Frohm, T. Cedervall, T.P.J. Knowles, T. Leiding, S. Linse
Communications Biology volume 2, Article number: 365 (2019)

II **Ultrastructural evidence for self-replication of Alzheimer-associated Aβ42 amyloid along the sides of fibrils**
M. Törnquist, R. Cukalevski, U. Weininger, G. Meisl, T.P.J. Knowles, T. Leiding, A. Malmendal, M. Akke, S. Linse
PNAS, in press

III **Secondary nucleation in amyloid formation**

M. Törnquist, T.C.T. Michaels, K. Sanagavarapu, X. Yang, G. Meisl, S.I.A. Cohen, T.P.J. Knowles, S. Linse
Chem. Commun., 2018, 54, 8667

IV **pH dependence of Aβ aggregation**

M. Törnquist, A. Dear, X. Yang, T.P.J. Knowles, S. Linse
Manuscript

V **Distinct thermodynamic signatures of oligomer generation in the aggregation of the amyloid-β peptide**
S.I.A. Cohen, R. Cukalevski, T.C.T. Michaels, A. Šarić, M. Törnquist, M. Vendruscolo, C.M. Dobson, A.K. Buell, T.P.J. Knowles, S. Linse
Nature Chemistry | VOL 10 | MAY 2018 | 523–53

My contributions to the papers

Paper I:

I participated in the experiments following kinetics at constant CSF concentration. I performed the testing and implementation of the automated dispenser. I performed the seeding experiments. I participated in data analysis and the writing and editing of the manuscript.

Paper II:

I prepared samples and collected data for all cryo-EM images except the first two datasets. I contributed to experiment design and data analysis and I took a major part in writing the manuscript with input from all authors.

Paper III:

I wrote the section on opens questions and outlook, I took part in editing the manuscript.

Paper IV:

I took part in designing the study, I performed the experiments that were included in the manuscript, I wrote the first draft of the manuscript.

Paper V

I performed the differential sedimentation experiments and *cryo*-EMimaging underlying the fibril size distribution estimates. I took part in the kinetic experiments at lower temperatures (10-14°C).

Acknowledgements

This work would not only have been impossible, but even unthinkable, without the support of some truly great people. First and foremost I must thank **Sara**, for letting me stay as a PhD-student in your group. You have always been available to discuss difficult experimental issues, thorny theoretical concept or just life in general. It has been a pure joy to come into the lab in the morning and see you already happily working on some new exciting experiment. I could not have asked for a better supervisor. A big thank you also to my co-supervisor **Tommy**, for always having a wise word to spare and for, together with **Susanna**, bringing new leadership to the CMPS. And of course, a big thank you to my co-co-supervisor and office mate **Thom**, thank you for involving me in your mad invention schemes, and for making our office a place for all sorts of interesting discussions (even when we really ought to be working).

Speaking of office mates, the third seat in our office has seen some fantastic people as well. **Xiaoting**, I miss your bizarre Chinese snacks and your cheerful company. I maintain to this day that England got better than it deserved when you moved there. **Anders**, working with you has been a true privilege and your easygoing helpfulness continues to cheer me up. **Björn** thank you for putting up with my constant random interruptions, for your spectroscopic insights and especially for turning the 3D-printer to use for the good of humanity.

Working in this group I have always felt that I was surrounded by friends. From the first moment when I was unexpectedly thrown into the mad world of amyloid research I had some very supportive people by my side. **Risto**, thank you for teaching me all your $A\beta$ trade secrets, and for discovering the fuzzy fibrils. **Kalyani**, thank you for your great cooking lessons, and for always giving me the feeling that things will work out, whether dealing with chaos in the lab or being lost in the streets of Edinburgh. Thank you also for always letting me borrow your buffers and various lab equipment, especially the ones I didn't tell you about (I put them back). **Ricardo** you were such a cheerful presence in the lab, always willing to help, I miss you. **Rebecca**, thank you for the much needed coffee in the sun, for many great talks and for the awesome paper we wrote together. I should also thank you for spotting the salary increment I missed, I believe I still owe you for that. **Tanja** thank you for being a lovely company during all the dissertation dinners, apparently "white amyloid parents" is a seating category, also thank you for bringing me hope that there is life after printing. **Tinna**, thank you for making what could have been a useless conference into such a memorable adventure and for always being a true friend to vent the hardships of amyloid life with. **Veronica**, out of all the Italians you are the Italianest, thank you for all the laughs and great times and for trying to keep my back straight, I'm afraid writing from home has not been kind to my posture. **Dev** thank you for all the nice chats,

I think we have jointly found that secondary nucleation and terrible lab reports are equally hard to eliminate. **Eimantas**, I am slightly disappointed that you didn't make it to PhD before me, I guess the race for professorship is on. **Egle** thank you for putting up with all of us while we jabber on endlessly about our amyloids, and **Lei**, for bringing new energy to the group and for building a machine that even I could almost not fail to operate. **Stefan**, you always had my back during teaching, your low-key irony is sorely missed. **Martin** thank you for keeping things running smoothly, I am sure I would be in debtors prison by now without your work. Thank you **Birgitta**, for patiently dealing with my missteps in the lab, and especially thank you for all the $A\beta$ you purified throughout the years. If I had kept all the fibrils I made from it I could have knitted you a sweater, except I can't knit and also that would have been horrible. A big thank you also to **Karin Åkerfeldt**, your presence in our lab always lifts our spirits.

Special mention also goes to **Alex, Georg** and all the people of the **Knowles lab** for truly brilliant collaborations, and to **Mikael** and **Uli** for continuously strengthening our manuscript and sticking to it through endless rounds of revisions.

I have had the privilege of acting as the supervisor for some great students, whose work has also been of value for this thesis. Thank you **Emelie** for your thorough work on the dispenser, also thanks to **Mattias** and **Elsa** for a very exciting project, even though the oligomer factory has yet to see the light of day. **Francesca**, thank you for bringing your dedication and energy to the pH 6.8 project, next you'll have to teach me everything you learned while I was busy writing.

The CMPS at large has been a very nice place to work in and a big thanks go out to all who made my lunches and fika-breaks so enjoyable, with special mentions to **Olof**, for making sure I attended those breaks and for giving me my very own theme song, **Filip** for sharing the pains of parenting and PhD-ing, **Veronika**, for your positive outlook, **Kristine** for always being polite when I pretend to understand your danish. Thanks also to the Pathfinder gang **Sven, Camille, CJ, Samuel** and **Mathias**, for continuing to demonstrate that the best laid plans can be turned into glorious flaming disaster. Special thanks to **Viktoria** and **Ben**, it has been a pure delight and I look forward to continued adventures. **Katja**, thank you for facing the most challenging mass-spec conundrums with your endless positivity and thank you **Cecilia** for your friendliness and your commitment to education. **Magnus** and **Maryam**, thank you for keeping this place running against all odds.

A big thank you also to **Paula**, without your dedicated work this book would have been a much shoddier production.

I first set foot in Lund University in the autumn of 2004, to the last ones standing of the old nano crew, **Johan** and **Björn**, thank you for that time and for still being

around. It has also been a much needed lifeline to sometimes hear from my friends outside the university, in that magical land where people don't live under the tyranny of anonymous reviewers. To the extended folkhögskola family, **Katta, Björn, John, Johanna, Maria, Erika, Sofia, Mandy, Katrin** and **Linnea**, thank you for reminding me that there is such a place. Speaking of other worlds, a very special thank you to my oldest friend and partner in crimes against reality, **Johan** for always being with me to talk endlessly about whatever our so similar but so different minds might conjure up.

As we will see in this book it is not always easy to tell cause from effect, and I am not sure if my interest in science was born solely from the endless summers reading through the entire science fiction collection of the Askersund library, but it certainly didn't hurt. To my dear **parents**, thank you so much for those summers and for all your support since. To my brother, **Rasmus** who has watched my academic path with a mixture of fascination and horror, thank you for always being there to complain over a beer about how dumb the world is, and thank you for the greatness that happens when our strange obsessive interests momentarily align. A special thanks to my beloved daughters, **Mira** and **Jonna**. You have been a welcome (usually) distraction (constantly) from the writing of this book and a vital reminder that there are times in life when the only sensible thing to do is to sit on the branch of a tree and eat an ice cream. And finally, a big thank you to my amazing and beautiful wife, **Kicki**. Our evening walks have been my one link to sanity during this very strange spring. No matter what comes next, I am so very lucky to have you by my side. I love you.

Populärvetenskaplig sammanfattning på svenska

För att sätta det här arbetet i sitt sammanhang måste vi börja med att prata om vår tids vanligaste demenssjukdom, Alzheimers sjukdom. Allteftersom fler människor lever till högre ålder blir Alzheimers allt vanligare och tyvärr finns det fortfarande inget botemedel. En stor del av problemet är att det fortfarande är väldigt mycket vi inte vet om hur sjukdomen verkligen fungerar. Alzheimers sjukdom leder till att nervceller dör och att den drabbade får allt värre problem med minnet och andra tilltagande kognitiva besvär. Exakt vad det är som dödar nervcellerna är fortfarande oklart, ett antal olika saker verkar gå fel i hjärnan i samband med sjukdomen men det är inte helt lätt att reda ut vad som är orsak och verkan. En av de misstänkta faktorerna är ett litet protein som kallas $A\beta$, och det kommer att vara huvudpersonen i den här boken. Det här proteinet finns i hjärnan även hos friska människor, exakt vad det är till för är en av de många saker vi fortfarande inte är säkra på. I samband med Alzheimers sjukdom så sker en förändring med $A\beta$ och det börjar bilda långa fibrer som i sin tur klumpas ihop och bildar plack inuti hjärnan.

För att få en uppfattning om hur en sådan fiber är uppbyggd, tänk dig ett enkelt torn av lego, där varje legobit motsvarar en proteinmolekyl. För att komma lite närmare verkligheten, föreställ dig också att de fria legobitarna är böjliga men att de låses fast i en viss form när de kopplas på tornet. För att undvika otillbörligt gynnande måste jag påpeka här att det även finns andra märken av modulära byggklossar, och på samma sätt finns det även ett stort antal andra protein som kan bygga upp den här typen av fibrer. De flesta är kopplade till någon form av neurodegenarativ sjukdom. Proteinerna alltså.

Det har visat sig att själva fibrerna i sig inte är speciellt farliga. Istället verkar det som att den skadliga formen uppstår någonstans på vägen, när $A\beta$ bildar former som består av fler än en kopia av proteinet, men som inte har fått den slutliga formen av en fiber. De här mellanformerna kallas med ett samlingsnamn för ”oligomerer”, och de kan uppträda i många olika former. Det pågår väldigt mycket forskning kring vilka typer av oligomerer som $A\beta$ kan bilda, och vilka av dessa som faktiskt har med sjukdomen att göra.

Men vi ska inte glömma bort fibrerna. Det visar sig nämligen att fibrer kan påskynda bildandet av oligomerer, varav vissa sedan går vidare och bildar nya fibrer. Den här processen, som vi på ren svenska kallar sekundärnukleering, leder alltså till en slags rundgång, om vi har lite fibrer så bildas det väldigt snabbt fler, som i sin tur bildar ännu fler. På vägen genereras det samtidigt skadliga oligomerer.

Eftersom det är möjligt att sekundärnukleering spelar en roll i Alzheimers sjukdom så går vårt arbete ut på att försöka förstå processen i så stor detalj som möjligt. Till

vår hjälp har vi en färgmarkör som ger en ljussignal när den binder till fibrerna och på sätt kan vi följa hur fibrer bildas i realtid. Genom att mäta hur hastigheten hos tillväxten ändras med olika betingelser kan vi dra slutsatser om hur processen går till på molekylnivå. Vi använder också olika typer av mikroskopi för att få en bild av hur fibrerna ser ut i olika stadier av processen, ibland med överraskande resultat.

Normalt sett, för att det ska gå att tolka resultaten, så sker de här studierna på ren $A\beta$ under väldigt kontrollerade förhållanden. Det är alltså en helt annan situation än den som råder inuti hjärnan, där det ofta kan vara ganska rörigt. För att komma lite närmare realistiska förhållanden har vi här också gjort experiment där vi tillsätter mänsklig cerebrospinalvätska (fråga inte) till våra experiment och bekräftar att fibrilbildningen sker på ett liknande sätt även då.

Vi har också gjort mängder av mätningar vid olika temperaturer och pH-värden, inte nödvändigtvis för att efterlikna betingelser inuti hjärnan, utan för att studera de grundläggande drivkrafterna bakom processen.

Tanken med allt detta är att att bygga en alltmer detaljerad bild av hur det går till när $A\beta$ bildar fibrer och oligomerer. På så vis kan vi bidra till en bättre förståelse av hur det här proteinet fungerar, som sedan, förhoppningsvis, kan öka chanserna att hitta ett sätt att bemöta Alzheimers sjukdom.

Chapter 1

Background

1 Alzheimer's disease

Alzheimer's disease (AD) is the most common form of dementia, causing massive neural damage, memory loss and eventually death. The risk of getting the disease increases sharply with increasing age, with an incidence of roughly 1% at age 80 and 5-10% at age 90 [1]. As our successes with combating other leading causes of death and disease has led to an increased life expectancy, an ever larger fraction of the population now lives to an age where the risk of AD is high [2–4]. In addition to age there are several life-style risk factors, including low education [5], lack of sleep [6], smoking [7], obesity [8, 9] and diabetes [10]. Addressing these risk factors can partially reduce the incidence of AD [11] but even then the total numbers can be expected to keep rising. There are also those who carry genetic risk factors, associated with a highly increased risk to get the disease, and sometimes with an early onset and rapid progression. There is thus a great need for an effective treatment and currently we have none. This has prompted a massive research effort into the underlying mechanisms of the disease in the search for some way to cure or at least delay it.

2 The amyloid cascade

One of the key pathological features of AD is the deposition of extracellular plaques and the formation of extracellular neurofibrillary tangles. The tangles are composed of a hyper-phosphorylated form of the microtubule associated protein Tau [12], while the plaques were identified to be mainly composed of an abnormally folded protein, Amyloid beta ($A\beta$) [13, 14]. $A\beta$ exists in a number of different length variants, res-

ulting from the cleavage of a large, transmembrane protein known as the Amyloid Precursor Protein (APP) [15]. The most common form of $A\beta$ is $A\beta 40$, while $A\beta 42$ is more prevalent in plaques[16], more aggregation prone and more cytotoxic[17].

In addition to its presence in the plaques there are several other factors that implicate $A\beta$ as a key player in AD, including the fact that persons with Down's syndrome, who carry an extra copy of chromosome 21 and thus overexpress APP have a significantly increased risk of developing AD [14]. There are also several examples where point mutations in the APP is linked to early onset familial AD [18–20]. This evidence, while not conclusive, has lended support to the amyloid cascade hypothesis. Essentially it posits that there is a direct causal link between deposition of missfolded $A\beta$and subsequent formation of neurofibrillary tangles, cell loss and dementia [21]. The hypothesis has been continually updated and refined [22], the largest modification being the finding that the end product of $A\beta$ deposition, the fibrils, seem relatively harmless, while species formed during the reaction are far more toxic [23]. The precise nature of this toxicity has not been conclusively determined, to a large extent because of the large variety of plausible toxic mechanisms that have been proposed. Some of the common examples include cell membrane pore formation[24–27], binding to specific nerve receptors [28, 29], and formation of reactive oxygen species [30–32]. Another suggestion is that $A\beta$ acts as an upstream initiator of other event, such as the hyper-phosphorylation and aggregation of Tau, which in turn leads to toxicity [33–36]. While the molecular nature of such is link still remains to be fully established, one very compelling candidate has been identified in the glycogen synthase kinase 3α, which has been shown to phosphorylate tau more rapidly in the presence of $A\beta$ oligomers [37].

3 Amyloid structure and organization

Amyloid fibrils are hierarchical assemblies with multiple levels of organization. The minimal unit of a fibril is called a filament and is built up by a large number of peptide units stacked perpendicular to the fibril axis. The stacked peptides are stabilized by intermolecular hydrogen bonds and thus form an extended β-sheet, responsible for the characteristic amyloid cross β diffraction pattern [38]. Each plane in a filament consists of one or more copies of the peptide, which pack into the fibril by taking up a specific fold, shared by every peptide in the fibril. In recent years structural studies have revealed a number of these folds, including two very similar structures that were determined for $A\beta 42$ using solid state NMR [39, 40], one of which [40] is depicted in figure 1.1. For $A\beta 40$, a large number of different structures have been reported [41–44], indicating that the same peptide is capable of taking on a range of different folds. Another layer of complexity is added by the fact that two or more filaments can be

laterally attached, and that this parallel stacking can happen in many different ways for the same fold [45–47]. Both these effects contribute to the commonly reported polymorphism of amyloid fibrils where within the same sample fibrils of very different morphology can be found [48]. The peptide fold, together with the filament stacking, will determine the surface properties of a fibril, which in turn dictates how it interacts with its surroundings.

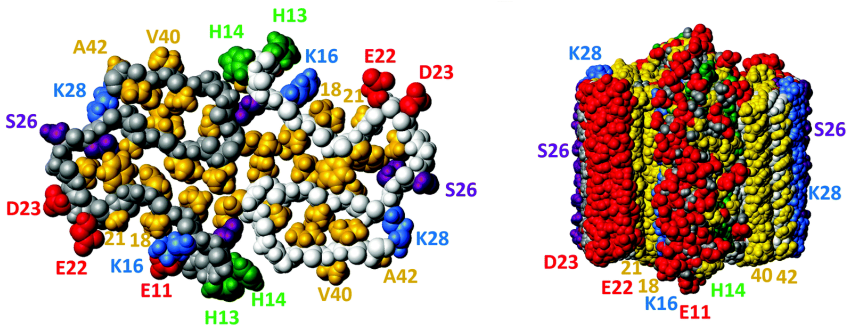

Figure 1.1: Structure of the peptide fold inside *Aβ*42 fibrils based on solid state NMR. Figure adapted from **Paper III**

Outside of the highly organized fibril form, amyloid proteins can also form a large variety of non-fibril aggregates, with a blanket term referred to as oligomers. These range from simple dimers, trimers and tetramers up to larger, globular assemblies. These various prefibrillar aggregates are almost uniformly reported to be cytotoxic [23, 49–51].

It also seems that some oligomers have the ability to link together to form 'beads-on-a-string'-like structures called protofibrils [52–54]. Both protofibrils and globular oligomers have been reported to convert to fibrils [51, 54, 55], or to have elements of the fibril structure [56]. There are also reports of oligomeric forms that seem to be incompatible with conversion to fibrils [57].

Chapter 2

The mechanism of fibril formation

1 Nucleated polymerization

In the past decade, the development of improved experimental techniques has expedited collection of reproducible data on the kinetics amyloid fibril formation [58–60]. At the same time, the analysis of this data has been greatly facilitated by the development of analytical kinetic models[60–62]. Integrated rate laws have been derived based on the microscopic steps that make up the aggregation pathway and their contributions to the overall rates. In this chapter we will walk through this process, with a focus on the microscopic steps and how they affect the overall reaction.

1.1 Primary nucleation and elongation

In amyloid aggregation, much like in writing, the very first step is the slowest. This is a feature that is common in many phase transitions, including freezing of water and formation of bubbles in a carbonated beverage. It is the result of the fact that the

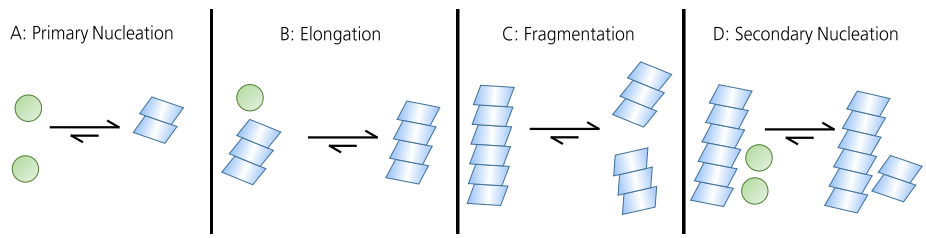

Figure 2.1: Principle sketches of the main mechanistic steps

smallest aggregates are inherently unstable, due to the large unfavourable free energy cost of creating a surface. On average they will therefore dissolve faster than they grow. However, at a certain size this tendency is reversed and further growth is favoured. The process of random assembly and disassembly until the barrier is overcome is referred to as **primary nucleation**, and the aggregate at the critical size is called a critical nucleus ((figure 2.1 A). In the case of amyloid aggregation, it is likely that the critical energy barrier to be overcome is associated with a structural conversion rather than simply achieving a specific size. Once a nucleus has formed it can continue to grow through **elongation** as new monomers add to the fibril ends and take on their structure (figure 2.1 B). Elongation has a lower energy barrier than nucleation and thus proceeds at a much higher rate.

1.2 Secondary processes

It is quite possible to have a reaction consisting of only nucleation and growth, but the aggregation patterns of most amyloids have features that are not captured by this simple model. This is manifested in a distinct lag phase, followed by a rapid acceleration of growth which suggests a mechanism by which the existence of fibrils accelerates the rate of further fibril formation. One such mechanism is **fragmentation**, the breaking of fibrils to create new growing ends (figure 2.1 C). This leads to a sharp increase in growth rate since the fibril ends are the site where new fibril mass is being generated through elongation. New fibril ends can also be generated by catalysis on the fibril surface (figure 2.1 D) in a process called **secondary nucleation**. This effect was first described for protein systems in the aggregation of sickle cell hemoglobin [63], but has been a well-known phenomenon in the crystallization of small molecules and proteins for decades [64]. Several pathogenic amyloid systems have been demonstrated to be heavily influenced by secondary nucleation, including $A\beta 42$, where it was found that the common practice of shaking the samples promoted fragmentation while quiescent conditions made it possible to observe the predominance of secondary nucleation [60]. Other examples are $A\beta 40$ [65], α-synuclein, [66], IAPP [67] and insulin [68]. In contrast, functional amyloids that build up bacterial biofilms do not have this growth profile because they employ imperfect repeats to counteract secondary processes [69]. It could be the case that the uncontrollable growth brought on by autocatalysis is inherently detrimental to living systems and is by and large selected against, the pathogenic amyloids representing border cases that are barely stable enough.

2 Rate equations

Having identified the possible steps in the reaction, we can now formulate in mathematical terms how the system might evolve over time. We will begin by defining some variables to describe the state of our system.

- $m(t)$ is the concentration of peptides that exist as free monomers.
- $M(t)$ is the corresponding concentration of peptides in the fibril state, also known as the mass concentration of fibrils.
- $P(t)$ is the number concentration of fibrils.

If we start from a pure monomer solution, $m(t)$ will have some initial value, m_0, while $M(t)$ and $P(t)$ will start at zero. Primary nucleation will generate new fibrils at a rate determined by the monomer concentration, $m(t)$, the primary nucleation rate constant, k_n, and the primary nucleation reaction order n_c.

$$\frac{\delta P}{\delta t} = k_n m(t)^{n_c} \tag{2.1}$$

Of course this process will also consume monomers and add to fibril mass, but this contribution is small enough to be neglected. The process that is mainly responsible for converting monomers to fibril mass is elongation which will do so with a rate determined by the concentration of fibril ends, $P(t)$, the elongation rate constant, k_e, and the monomer concentration, $m(t)$.

$$\begin{aligned} \frac{\delta M}{\delta t} &= k_e m(t) P(t) \\ \frac{\delta m}{\delta t} &= -k_e m(t) P(t) \end{aligned} \tag{2.2}$$

Fragmentation of fibrils will significantly increase the rate of aggregation by creating new growing ends at a rate proportional to the total fibril mass, $M(t)$, and the fragmentation rate constant, k_f.

$$\left(\frac{\delta P}{\delta t}\right)_{\text{frag}} = k_f M(t) \tag{2.3}$$

Secondary nucleation, finally, leads to a generation of new fibrils, and thus new growing ends, that depends on the secondary nucleation rate constant k_2, the monomer

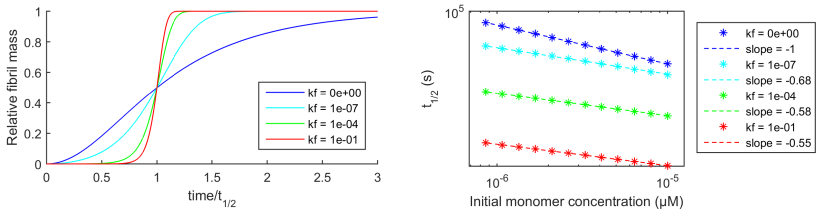

(a) Variations in curve shape by increasing k_f (b) Shift in monomer concentration dependence by increasing k_f

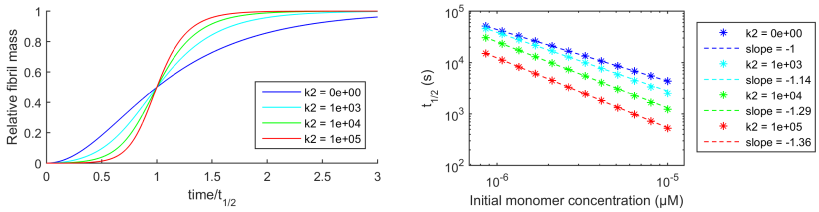

(c) Variations in curve shape by increasing k_2 (d) Shift in monomer concentration dependence by increasing k_2

Figure 2.2: Numerical simulations of fibril formation in different regimes.

concentration, m(t), the secondary nucleation reaction order, n_2 and the fibril mass M(t):

$$\left(\frac{\delta P}{\delta t}\right)_{sec} = k_2 m(t)^{n_2} M(t) \tag{2.4}$$

The contributions of these different processes add up to create a differential equation system that describes the time evolution of the fibril formation process. We can use this to investigate how changing the influence of the different microscopic steps affect the overall process, as shown in Figure 2.2. Panel (a) shows how the shape the of the aggregation curve changes as we go from a reaction with only primary nucleation and elongation (blue curve) to reactions with increasing rates of fragmentation (cyan, green and red curves). Panel (c) shows the same for increasing rate of secondary nucleation. In both cases the introduction of a secondary process creates a steeper aggregation curve. Panels (b) and (d) show the time it takes for half of the monomers to become incorporated into fibrils, denoted $t_{1/2}$, as a function of initial monomer concentration. The dotted lines represent a power function on the form:

$$t_{1/2} = A * m_0^{\gamma} \tag{2.5}$$

The scaling exponent, γ, describes how the rate of fibril formation depends on the

monomer concentration. This makes it possible to quickly assess which microscopic steps are of importance under a given set of conditions. In the case of fragmentation, its rate does not depend on the monomer concentration, which leads to an overall decrease in the monomer dependence of the reaction. This shows up in the flatter $t_{1/2}$-curves and decrease of $|\gamma|$. Secondary nucleation on the other hand is strongly dependent on the monomer concentration and thus gives the opposite effect, with steeper $t_{1/2}$-curves and increasing $|\gamma|$.

2.1 Integrated rate law

In the end we want to arrive at a means to determine the individual rate constants, k_n, k_e, k_f and k_2, in order to quantify the contributions of the different microscopic processes. To facilitate this, the rate equations have been solved to create a single master equation that describes the time evolution of fibril mass [70]:

$$\frac{M(t)}{M_\infty} = 1 - \left(\frac{B_+ + C_+}{B_+ + C_+ e^{\kappa t}} \cdot \frac{B_- + C_+ e^{\kappa t}}{B_- + C_+} \right)^{\frac{k_\infty^2}{\kappa k_\infty}} e^{-k_\infty t} \tag{2.6}$$

where

$$\begin{aligned} \lambda &= \sqrt{2 k_+ k_n m(0)^{n_c}} \\ \kappa &= \sqrt{2 k_+ k_2 m(0)^{n_2+1}} \\ B_\pm &= (k_\infty \pm \tilde{k}_\infty)/(2\kappa^2) \\ C_\pm &= \pm\lambda^2/(2\kappa^2) \\ k_\infty &= \sqrt{2\kappa^2/[n_2(n_2+1)] + 2\lambda^2/n_c} \\ \tilde{k}_\infty &= \sqrt{k_\infty^2 - 4 C_+ C_- \kappa^2} \end{aligned} \tag{2.7}$$

Using this equation, and expansions of it, it has been possible to extract the individual rate constants and how they change with conditions, and thus gain insights into the aggregation mechanism. To facilitate this the online platform Amylofit was developed, allowing large datasets to be uploaded and anlayzed by globally fitting the models to the entire dataset and estimate the parameters [61].

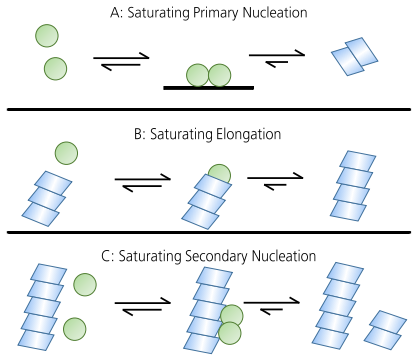

Figure 2.3: A: Heterogeneous primary nucleation may saturate as the available surfaces become increasingly covered.
B: Multi-step elongation may saturate as the fibril ends become increasingly occupied.
C: Multi-step secondary nucleation as the fibril surfaces become increasingly covered.

3 Saturation

3.1 Microscopic steps can be saturated

One of the early indications that secondary nucleation is an important contributing factor was the monomer concentration dependence, described by the scaling exponent. However, in several conditions it was observed that the scaling exponent changes with monomer concentration, indicating saturation of secondary nucleation. This was observed for $A\beta 40$ [65], but also for $A\beta 42$ at pH 7.4 [71] and at high ionic strength [72]. In both experiment [65] and simulations [73] it seemed like the rate of secondary nucleation depends on the fractional surface coverage of fibrils, making it scale with concentration similarly to what is seen in Michealis-Menten kinetics, as catalysis is preceded by the formation of a relatively long-lived enzyme-substrate complex [74]. All monomer dependent steps can in principle be saturated in analogous ways. Primary nucleation has been seen to saturate in the case of $A\beta 40$ at pH 7.4 [62]. This saturation is most probably the result of heterogeneous primary nucleation (figure 2.3 A) where the catalytic surface might be the air-water interface or the inside of the reaction container. Even though there are many conditions where saturation of primary nucleation is not observed it is very likely that the nucleation is surface catalyzed also in those cases, only not to an extent that leads to detectable saturation. Several studies have shown that elongation seems to be a multi-step reaction involving attachment to the fibril end followed by a conversion step where it takes up the structure of the fibril [75–78] (figure 2.3 B).

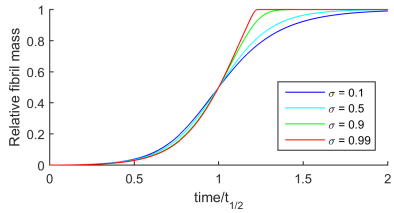

(a) Effect on curve shape as k_e saturates

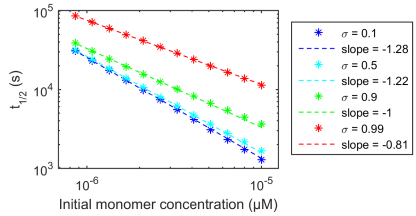

(b) Effect on $t_{1/2}$ shape by saturation of k_e

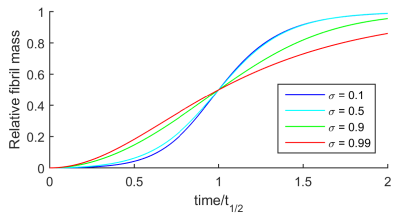

(c) Effect on curve shape as k_2 saturates

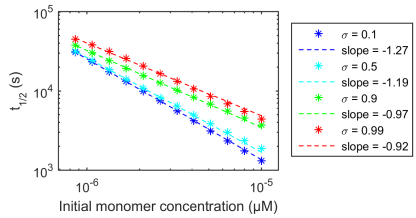

(d) Effect on $t_{1/2}$ shape as k_2 saturates

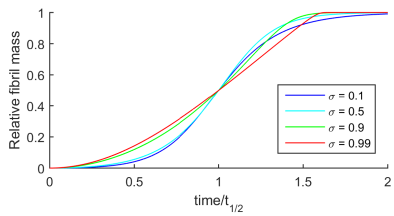

(e) Effect on curve shape as k_e and k_2 saturates

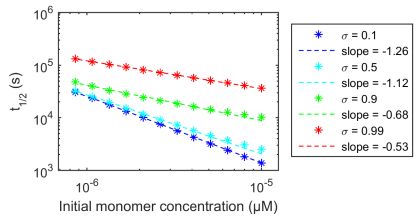

(f) Effect on $t_{1/2}$ shape as k_e and k_2 saturates

Figure 2.4: Numerical simulations of fibril formation as various processes are saturated.

3.2 A model of saturation

Saturation of microscopic steps can be accounted for using an analogy of Michaelis-Menten kinetics (see box). In this, the rate constants of each process are replaced by effective rate constants as follows:

$$\begin{aligned} k_n' &= k_n \frac{K_P^{n_c}}{1 + K_P^{n_c}} \\ k_+' &= k_+ \frac{K_E}{1 + K_E} \\ k_2' &= k_2 \frac{K_S^{n_2}}{1 + K_S^{n_2}} \end{aligned} \tag{2.8}$$

Here, K_P, K_E and K_S associated with the respective rate constants are analogous to

the Michealis constant in that they are related to the affinity between the substrate and the catalytic surface. These modified rate constants form the basis of a newly derived version of the integrated rate law [62] :

$$\frac{M(t)}{M_\infty} = 1 - \left[1 + \frac{\epsilon'}{c'}\left(e^{\kappa' t} + e^{-\kappa' t - 2}\right)\right]^{-c'} \tag{2.9}$$

where

$$\begin{aligned} \epsilon' &= \frac{k_n' m_{tot}^{n_c}}{2k_+' k_2' m_{tot}^{n_2+1}} \\ \kappa' &= \sqrt{2k_+' k_2' m_{tot}^{n_2+1}} \\ c' &= \frac{3}{2n_2' + 1} \end{aligned} \tag{2.10}$$

The value of the affinity constants can change, both with peptide sequence and with solution conditions, which will affect whether saturation effects are observable in a given concentration span. Only if the value of K_P, K_E or K_S fall inside the examined concentration span can it be determined with any accuracy. If it is significantly below the lowest concentration the process will be saturated through the whole range.If it falls well above the highest concentration no signs of saturation will be detectable, as is the case for $A\beta 42$ at pH 8.0.

4 What happened to the oligomers?

The attentive reader might have noticed that, for all our talk of oligomers in the previous chapter, there is no mention of them in the model. The reason is that even though the model describes multi-step processes, we do not explicitly add in all the steps. Primary nucleation, for example, might require several stages of oligomerisation and rearrangement, but the rate constant k_n only reports on the net rate of formation of growth competent species. Various intermediate forms created along the way are only present in the model by their influence on the net rate. The same is true for secondary nucleation.

Chapter 3

Methods

1 Considerations when working with Aβ

The infamous difficulty in acquiring reproducible results with $A\beta$ aggregation once earned it the moniker "the peptide from Hell". It might be more accurate to describe it as the molecular equivalent of the Princess and the Pea. As long as it is payed attention to and doted on it behaves amiably, but even the tiniest perturbation might alter the outcome of an experiment. In the last decade we have seen that by carefully controlling some key aspects of the reaction conditions this chaotic streak can be managed [59].

Figure 3.1: *"The problem seems to be this green seed-pod stuck in the transport mechanism"*
Public domain illustration by Alfred Walter Bayes

- Purity: The kinetics are extremely sensitive to the molecular purity of the sample, even minute traces of contaminant proteins can disturb it. To alleviate this we express the peptide recombinantly and purify it from inclusion bodies using ion exchange chromatography and several rounds of size exclusion chromatography. The purity of the final product is confirmed with SDS-Page, mass spectrometry and finally we confirm that it gives reliable kinetics at the standard condition (pH 8.0, 20 mM phosphate) before using a batch for further experiments.

- Well defined starting conditions: In order to get meaningful kinetics steps must be taken to ensure that the starting state is pure monomer. That means that the purified peptide is dissolved in 6 M GuHCl and the solution run on a size exclusion column, the monomer peak collected, immediately placed on ice and used within a few hours. All solutions must be kept on ice at all times until the start of the experiment.

- Surfaces: Since $A\beta$ is very surface active it is important to control what types of surfaces it is exposed to. For normal kinetic experiments we always use low-binding, PEG-coated plates (Corning 3881) which have been found allow for reproducible kinetics. In other experiments it is sometimes necessary to use other types of reaction vessels, which tends to put the aggregation on a different time scale and impair reproducibility.

- Careful handling - The sensitivity of primary nucleation to surfaces, and of secondary nucleation and fragmentation to shear forces, also mean that careful handling of the samples in all stages is of importance. This includes careful pipetting to avoid the introduction of bubbles and to minimize shear forces. This has proven especially challenging when dispensing solutions into deep NMR tubes.

- Sample homogeneity: Many techniques pertaining to amyloid samples, both analytical and preparative, assume that the protein concentration is homogeneous throughout the sample. Unfortunately this is rarely the case for $A\beta$. Amyloid fibrils, once formed, will tend to aggregate into higher order assemblies. In *cryo*-EM samples of $A\beta$ fibrils are often found in spherical clusters that can be a few µm in diameter. In addition the fibrils tend to associate into clusters that can get to large enough to be observable with the naked eye.

2 Thioflavin t

Apart from the actual amyloid proteins, Thioflavin t (ThT), is perhaps the most important molecule to the amyloid field. Initially used to stain amyloid material in tissues [79], it has become the workhorse of amyloid kinetics after it was reported that it can give a fluorescent signal proportional to the fibril concentration [80]. The ThT molecule (Figure 3.2 (a)) consists of a benzothiazole ring and a benzyl ring connected by a single carbon-carbon bond. In solution, the two rings can rotate freely with respect to each other, allowing the molecule to dissipate energy and lowering the fluorescence quantum yield. As ThT binds to amyloid fibrils the rings are locked into place and the quantum yield increase (Figure 3.2 (b)).

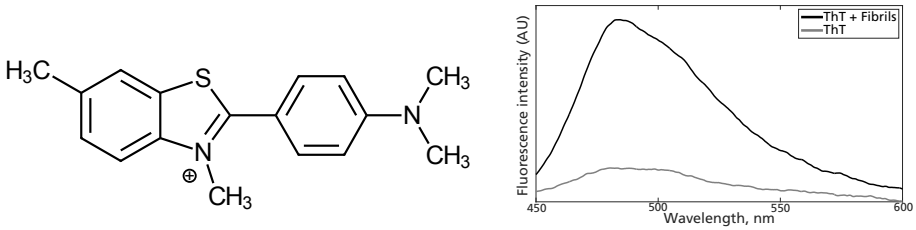

(a) (b)

Figure 3.2: (a): The structure of the Thioflavin T molecule. (b):The fluorescence spectrum of Thioflavin T alone (grey line) and in the presence of $A\beta 42$ fibrils (black line).

If the assay is properly calibrated the fluorescence response is proportional to the total fibril mass [59, 60]. However, there are cases where the presence of ThT itself may interfere with the aggregation kinetics [81, 82] or where some aspect of the experimental setup affects ThT fluorescence rather than the fibril formation. For each case it is therefore important to confirm findings based on ThT fluorescence with independent methods, and in general to have a good understanding of the experimental system [83].

3 NMR

Nuclear magnetic resonance (NMR) spectroscopy is a very powerful technique with a vast number of variations that can give information of molecular structures and dynamics. On the most fundamental level, NMR spectroscopy employs a very strong magnetic field to induce an enhanced energy difference between the spin states of nuclei in the sample. This difference can be probed by a radio-frequency pulse. Each nucleus in the sample contributes to a peak at the frequency that corresponds to the energy difference between its spin states. Since the nuclei are partially shielded from the external magnetic field by the surrounding electrons the energy differ-

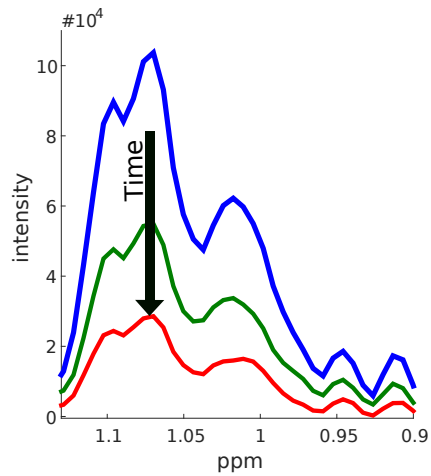

Figure 3.3: Example of NMT spectra collected from a sample of $A\beta 42$ at different time points. The depletion of monomer is detected as a uniform loss of intensity.

ence, and hence the peak position in the spectrum, is shifted by the particular chemical environment of each nucleus, an effect which is aptly named the *chemical shift*. The specific pattern of chemical shifts in a molecule contains a wealth of chemical and structural information and can also be used as a fingerprint to differentiate molecules in a sample.

NMR spectroscopy can be used follow amyloid aggregation. The intensities of the peaks with the chemical shift known to represent the methyl protons of the peptide are integrated to get a measure of the protein concentration in solution. Over the course of the aggregation reaction the peptide monomers are depleted from solution and thus the intensity is reduced (Figure 3.3). By collecting spectra at intervals over a time course the kinetics of monomer depletion can be tracked. This technique is a powerful complement to the ThT assay, as it is label free and gives information on a different aspect of the aggregation process, monomer concentration as opposed to fibril mass concentration. The main limitations are that it is typically limited to one sample at a time and that relatively high protein concentrations are required to get a sufficient signal.

4 cryo-EM

In transmission electron microscopy an image is created by shooting a high energy electron beam through a sample and measuring the transmitted electrons. In order for this to be possible the sample must be solid and very thin and be kept at low temperature and in a high vacuum. *cryo*-EM allows liquid samples to be analyzed in TEM by freezing them in a thin slab at ultra-low temperatures. The sample is first deposited on a thin carbon film with a large number of holes, mounted on a copper grid. The sample is then carefully blotted to remove excess fluid and rapidly plunged into a bath of liquid ethane. This rapid freezing is required to avoid the formation of crystalline ice that would otherwise interfere with imaging. The rapid freezing also allows components of the samples to be frozen in place with minimal perturbations before imaging, providing a snap-shot of the process under investigation.

5 Automated creation of dilution series

Out of the previously mentioned need for controlled and reproducible sample preparation was born the idea of an automatic dispenser to set up concentration series. While there are many commercially available pipetting robots none of them worked in quite the way needed to create dilution series for aggregation assays, so in the end

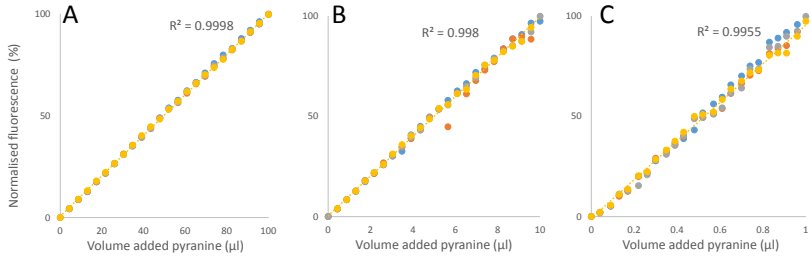

Figure 3.4: Linear dilution series of fluorescent dye made by the GraDis dispenser robot. The highest volume of dispensed dye solution going from 100 to 0 µl with steps of 4.3 µl (A), 10 to 0 µl with steps of .43 µl(B), 1 to 0 µl with steps of 0.04 µl (C), into a total volume of 100 µl.

one was constructed in-house. The device, called GraDis, consists of two step-motor controlled syringes which are connected to a dispenser head mounted on a movable arm. The user can design a desired concentration series to be dispensed into a 96-well plate.

Before GraDis was used for amyloid aggregation kinetics a large number of test rounds were performed using a fluorescent dye, pyranine, confirming that the delivered concentrations were accurate and reproducible. After several rounds of optimization and troubleshooting the dilution series in figure 3.4 could be produced, showing that the resulting concentrations retained linearity even when the dispensed volumes differed by as little as 40 picoliters.

Chapter 4

Discussion of the papers

Here we will take a closer look at the papers and discuss some of the main findings within, with a focus on how they add to our understanding of secondary nucleation. In **Paper I** we follow aggregation kinetics in human cerebrospinal fluid, showing that secondary nucleation remains a significant part of the aggregation mechanism in this complex environment. In **Paper II** we use NMR and *cryo*-EM to uncover an intermediate state were fibrils are transiently covered in dense, non-fibril protrusions, which seem to be the result of heavily saturated secondary nucleation. In **Paper IV** we follow aggregation kinetics over a wide range of pH, showing that decreasing pH seems to lead to saturation not only of secondary nucleation but also of other microscopic steps. In **Paper V** we follow aggregation kinetics over a span of different temperatures to determine the thermodynamic signatures of the different microscopic steps. Remarkably, we find that the energy barriers in secondary nucleation has a distinct profile from those of elongation and primary nucleation, a fact which might stem from the influence of fibril surface coverage. Since **Paper III** did not contain any novel data, but rather summarized our understanding at the time and ended with a number of open questions I will save that for the next chapter.

1 Paper I

The highly idealized conditions typically used to generate accurate and reproducible aggregation kinetics are a far cry from the highly complex environment where $A\beta$ aggregates *in vivo*. In the biological setting there is a myriad of other proteins at very high concentrations, leading to molecular crowding and a wealth of potential interaction partners. Surfaces, mostly in the form of lipid walls of cells and organelles, are also ubiquitous. In addition, various ions are present at high concentrations. All of these factors are known to affect the aggregation pathway of $A\beta$ to various degrees, and they all add up to a net effect which is effectively impossible to predict. In order to bridge this gap and connect the findings made *in vitro* to biologically relevant conditions we performed a series of experiments where we followed the aggregation of $A\beta 42$ in human cerebrospinal fluid (CSF).

We established that $A\beta 42$ does aggregate in CSF and that the aggregation, like in buffer, gives a measurable ThT signal. *cryo*-EM experiments confirmed that fibrils were formed with a morphology similar to those formed in pure buffer.

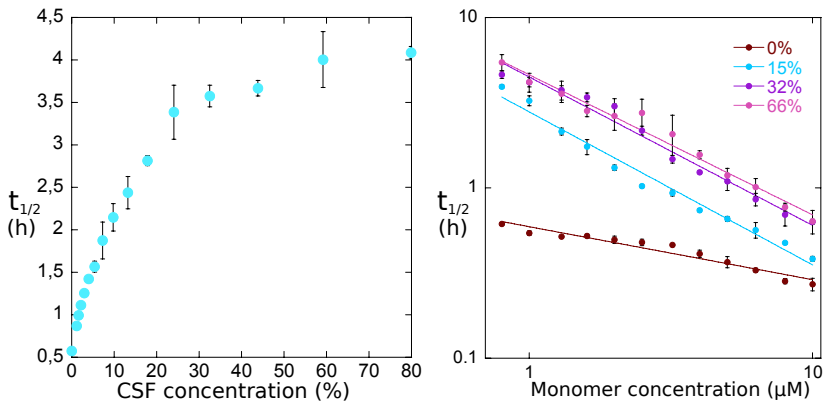

Figure 4.1: Left: $t_{1/2}$as a function of increasing CSF concentration. Right: $t_{1/2}$ as a function of $A\beta 42$ concentration at four different concentrations of CSF.

The effect of increasing percentage of CSF on the aggregation rate of a fixed $A\beta 42$ concentration was measured. The $t_{1/2}$ of the reaction increased with increasing CSF concentration, showing that the net effect of all components in CSF was retarding fibril formation. The precise pattern of this retardation varied between batches of CSF, some displaying a smooth increase reminiscent of a Langmuir binding isotherm (Figure 4.1, left), others having a less coherent appearance, but in all cases the overall trend persisted.

In order to assess the more detailed effects on the mechanism we also performed a series of experiments at constant CSF concentration and varying initial concentration of $A\beta$ monomer. The concentrations of CSF were chosen, based on the previous experiments, to be 0%, 15%, 32% and 66%. The buffer conditions were chosen to allow the buffer to be mixed with CSF in different ratios without creating any major shifts in ionic conditions. We thus used 140 mM NaCl and 1 mM $CaCl_2$. Hepes was used as a buffer to avoid the tendency for precipitation with Ca^{2+} associated with phopshate buffers.

Again the overall aggregation rate decreased with increasing concentration of CSF (Figure 4.1, right). When analyzing the data using the global fitting methodology described in Chapter 2 we found that the the model based on saturating secondary nucleation provided the best fit to the data at all CSF concentrations. Curiously, the most challenging condition from a data analysis perspective was the pure buffer, in order to achieve acceptable fits for this condition the reaction order of primary nucleation, n_c, had to be set to effectively 0. In other words, it seems like primary nucleation was fully saturated in this condition, which sets it apart from the previously studied systems, but the cause of this effect is not completely clear. The increased ionic strength could be partially responsible, as investigations at this and higher ionic strength has shown that secondary nucleation becomes increasingly more saturated, but reported no signs of saturation of primary nucleation [72]. Another possible candidate is calcium since studies have found it to accelerate amyloid aggregation [84].

In all conditions the affinity constant for secondary nucleation, K_S, (in the paper given as K_M, since at the time it was the only affinity constant under consideration) is well below the lowest $A\beta$ concentration used in the study. This means that we cannot get an accurate measure, either of K_S or k_2, the rate constant of secondary nucleation, but only their product. Because of this we cannot completely disassemble the effects of CSF on the secondary nucleation, but the general trend is a decrease in the effective secondary nucleation rate with the addition of CSF.

In conclusion we note that $A\beta 42$ aggregates in CSF and forms fibrils following kinetics that can be described by the same mechanistic model as has been established in a pure buffer system. Secondary nucleation remains a major source of new fibrils, albeit at a reduced rate. The system starts off heavily saturated and grows less so with the addition of CSF which is in agreement with the effects of a competitive inhibitor. These findings can help to focus the design of experiments to identify the various molecular components responsible for these effects.

2 Paper II

This project started out with the aim to follow the consumption of $A\beta 42$ monomers using NMR spectroscopy, as a complementary method to the standard ThT fluorescence assay. The overall trend, unsurprisingly, was that the monomer was depleted from solution at a rate that increased with decreasing pH (Figure 4.2. However, at pH 6.8 a curious effect appeared, the aggregation started off fast, only to slow down after approximately 10 h and the speed up again after 20 h. This behaviour was further accentuated with decreasing pH, with a very sharp initial drop followed by a slow drift towards the baseline. In order to get a better picture of what might be happening, samples were withdrawn from the ongoing reaction at pH 6.8 and investigated with *cryo*-EM. Samples were taken after 10 h and 30h, to investigate the beginning of the first plateau and the end state. The images from the 10 h sample revealed a second surprise, a dense covering of curly filaments protruded from the surface of all fibrils. In the end state the protrusions were gone and only typical amyloid fibrils could be found.

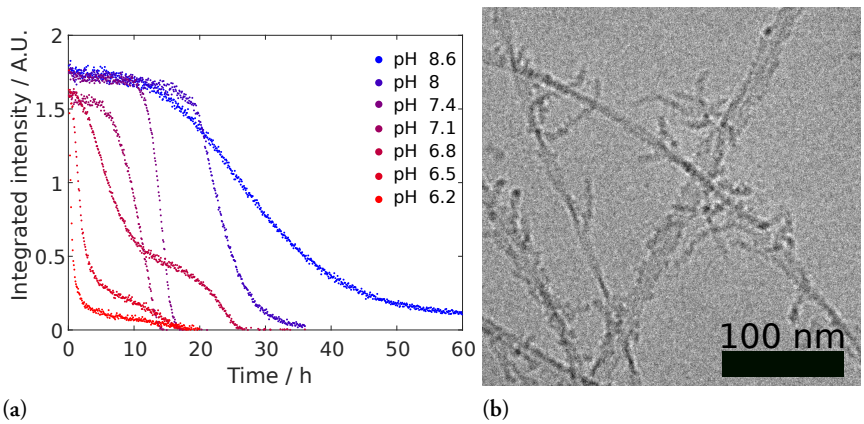

Figure 4.2: (a): $A\beta 42$ monomer concentration over time as monitored by NMR signal intensity at different pH (b):*cryo*-EM image taken after 2h at pH 6.8

In a series of follow up experiments additional time points were collected. It was found that the protrusions can be observed as early as after 2 hours but with less dense coverage. When studying the reaction in the presence of the chaperone domain Brichos, known to inhibit secondary nucleation [85], the surface coverage was markedly decreased and instead a large number of free-floating oligomers were observed. In a set of seeding experiments, where we added $A\beta 40$ fibrils to $A\beta 42$ monomers, the degree of coverage was also decreased, in keeping with the established absence of surface nucleation between $A\beta 40$ and $A\beta 42$ [86]. We finally attempted to seed the solution with

fibrils of $A\beta$(M1-42) that had been truncated using the GluC protease, yielding peptides of $A\beta$(12-42). With these seeds again the surface coverage seemed diminished, suggesting that the N-terminal part plays a role in attachment.This too, is in keeping with other studies, where altering the sequence of the N-terminal part of $A\beta$ has a marked effect on secondary nucleation [87]. Overall we could see that the surface coverage was diminished in conditions of suppressed secondary nucleation.

Putting the findings in the perspective of our earlier description of multi-step secondary nucleation it seems quite probable that the structures observed here are the result of heavy saturation. As the pH decreases the net charge of the $A\beta$ peptide is also reduced (less negative), leading to weaker electrostatic repulsion and giving the monomers a higher affinity for the fibril surface. Based on the appearance of the buildup on the fibril, it is likely that the process is stalled after oligomer formation but before detachment and structural conversion. Gaining further insights into the structure of the attached oligomers would do much to clarify this picture, especially if they could be compared with any of numerous other prefibrillar aggregates that have been reported.

There is also ongoing methods development to find a more quantitative method to follow the growth and disappearance of these intermediate structures. The aim is to investigate a range of different fluorescent probes, called luminescent conjugated oligothiophenes (LCOs) that have been reported to have differential affinities to different species throughout the aggregation pathway [88–90]. With a more facile and quantitative approach to complement the *cryo*-EM experiments we aim to continue elucidating the determinants and time evolution of this phenomenon.

3 Paper IV

This study aims to systematically investigate how the aggregation mechanism of $A\beta 42$ changes as a function of pH. The approach is similar to previous work on the effects of ionic strength [72] where the fibril formation process was followed across a wide span of NaCl concentrations. The motivation comes partly from the direct interest in the mechanism of fibril formation in mildly acidic conditions, as these might be relevant to the *in vivo* aggregation of $A\beta$, due to the link between $A\beta$ aggregation and the endo-lysosomal pathway [91–94].

The other aim is to extend the general mechanistic understanding of the fibril formation process. Several previous studies have already shown that $A\beta$ forms aggregates faster at lower pH [95–100]. There have also been findings showing an increased toxicity from those aggregates [101]. By altering the pH step-wise we hope to build a continuous mechanistic map from the well-known mechanism at pH 8.0 [60] to conditions where our current understanding is limited. Hopefully, other difficult to understand cases could then be placed on this map, allowing us to further connect up the previously so disjointed landscape of amyloid aggregation.

Table 4.1: The scaling exponent, γ, calculated from $t_{1/2}$in figure 4.4A

pH:	6.0	6.5	7.0	7.5	8.0	8.5
γ:	-0.10	-0.50	-0.55	-0.68	-1.25	-1.13

The initial experiments have consisted of unseeded kinetics of $A\beta 42$ aggregation, carried out at six different pH values, ranging from pH 6 to pH 8.5. By and large, we found and overall increase of the rate of aggregation with decreasing pH. This was accompanied by a flattening of the monomer concentration dependence, as reported by $t_{1/2}$, (Figure 4.4A, table 4.1) suggesting that saturation effects become more prominent. Especially at pH 6.0, with a γ of -0.1, the monomer concentration of $t_{1/2}$ is almost completely gone. There are also effects on the curve shape, at pH 6.5 the highest concentrations have almost identical slope and lag phase, leading to an overlap of the curves. Since monomer seems to be consumed at the same rate, and in the higher concentrations there is more total monomer to start with, this means that at the higher concentrations it actually takes longer to complete the reaction (Figure 4.3B) leading to an upturn in the $t_{1/2}$-curve (Figure 4.4B). At pH 6, the curve shape is more perplexing. Over the time course of the aggregation the slope of the ThT-curve decreases significantly, an effect that would normally be interpreted as a strong dependence on monomer concentration (Figure 4.3C). However, since the rate of the different reactions scales very weakly with initial monomer concentration, some other effect must be in play here. It is interesting to compare with work done on a

different amyloid system, GLP-1, where a very similar kinetic profile was observed in a pH-dependent manner, and was linked to the rapid early formation of a high concentration of oligomers [102]. Comparing also with our previous studies on $A\beta 42$ monomer depletion in **Paper II**, we see there a very rapid initial drop in monomer concentration followed by a slow depletion of the last portion over the course of several hours.

The effects seen this far can mostly be rationalized in terms of saturation effects brought on by an increased affinity of monomers for the various catalytic surfaces as electrostatic repulsion is reduced. Future experiments will be aimed at further dissecting these effect. Surface binding experiments with SPR can give independent measures of the surface affinity constants and mass spectrometry and size exclusion chromatography, possibly in conjunction with cross-linking could be employed to investigate early oligomer populations.

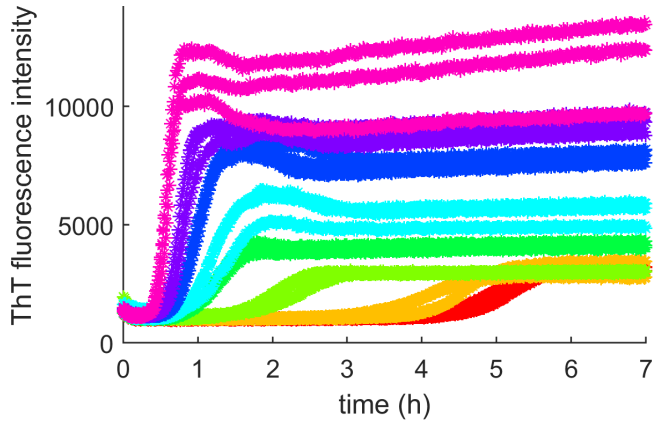

(a) pH 8.0

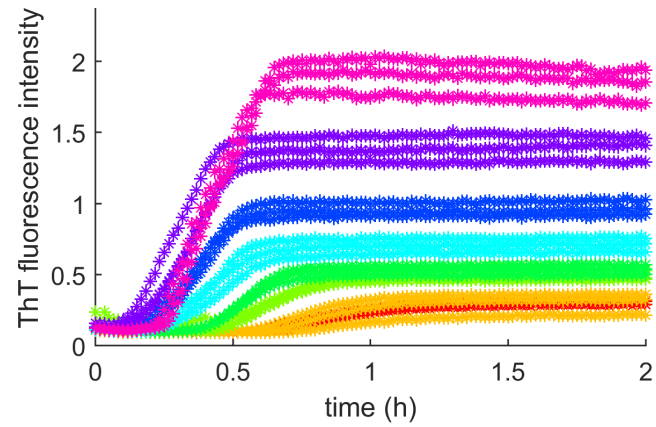

(b) pH 6.5

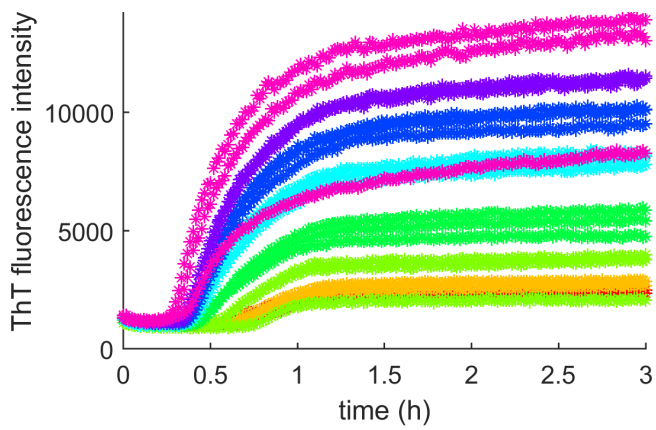

(c) pH 6.0

Figure 4.3: ThT fluorescence curves at three different pH. Initial monomer concentrations are 0.8, 1.1, 1.4, 1.9, 2.5, 3.5, 4.5 and 6 μM.

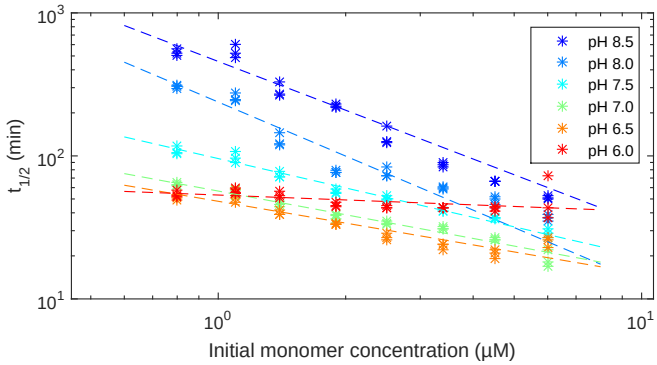

(a) $t_{1/2}$ as a function of monomer concentration at the 6 different pH values. Fitted curves on the form $t_{1/2} = \alpha * c^{\gamma}$

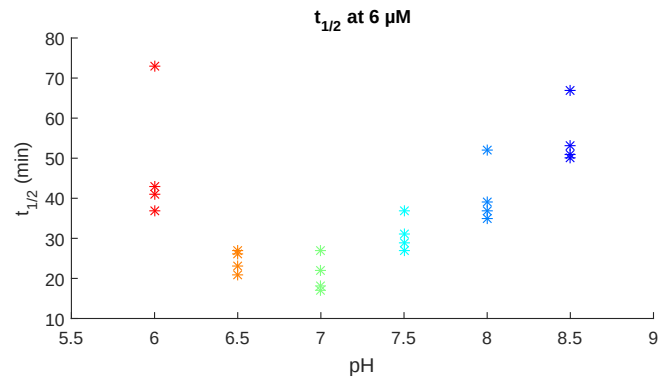

(b) $t_{1/2}$ as a function of pH at 6 μM initial monomer concentration.

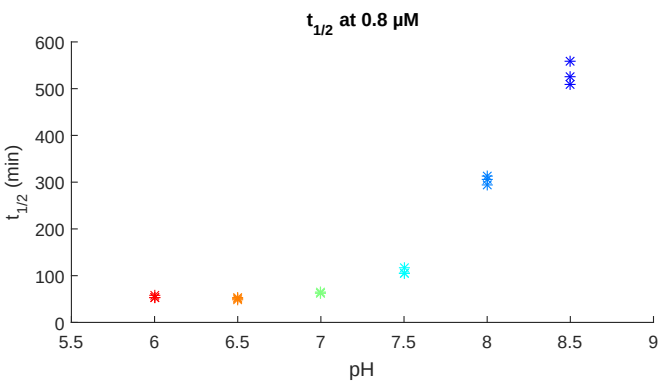

(c) $t_{1/2}$ as a function of pH at 0.8 μM initial monomer concentration.

Figure 4.4: Summary of $t_{1/2}$as a function of concentration and pH

4 Paper V

In this work the fibril formation of $A\beta 42$ was studied at a range of different temperatures in order to determine the temperature dependence, and thus the energy barriers, of the microscopic steps, primary nucleation, secondary nucleation and elongation. Using a combination of seeded and unseeded kinetics the individual rate constants, k_e, k_2 and k_+, could be determined at each temperature.

The temperature dependence of a rate constant is expected to follow the Arrhenius equation:

$$k = A \exp\left(-\frac{\Delta G^{\ddagger\Theta}}{RT}\right) \tag{4.1}$$

where A is a prefactor, R is the universal gas constant, T is the temperature an $\Delta G^{\ddagger\Theta}$ is the height of the highest energy barrier along the reaction pathway compared to the initial state. From this the contributions from enthalpy, $\Delta H^{\ddagger\Theta}$, and entropy, $\Delta S^{\ddagger\Theta}$, could be determined using $\Delta G^{\ddagger\Theta} = \Delta H^{\ddagger\Theta} - T\Delta S^{\ddagger\Theta}$.

As might have been expected, the overall rate of aggregation increased with increasing temperature. As can be seen in figure 4.5 this was the result of an increase in the rate constants of primary nucleation and elongation. The rate constant for secondary nucleation, in contrast, displayed a very flat dependence on temperature. When extracting the energy barrier components (listed in table) it is revealed that while both k_n and k_+ are associated with an enthalpic barrier while being favoured by entropy, the reverse is true for k_2 (Table 4.2). The increased relative influence of secondary nucleation becomes strikingly visible when comparing the shapes of the curves generated at the same concentration at different temperatures (Figure 4.6). As the temperature is decreased, the lag phase becomes much longer, but once the reaction takes off the increase is very sharp.

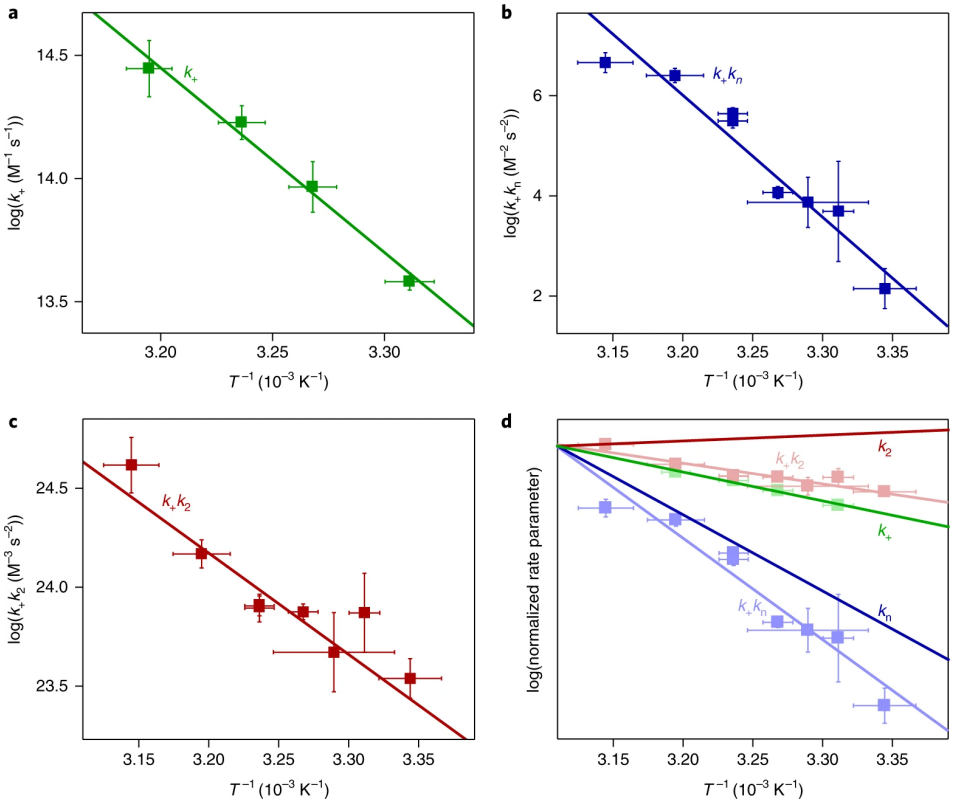

Figure 4.5: Arrhenius behaviour of the microscopic rate constants for $A\beta 42$ aggregation. **a:** k_+ as determined by heavy seeding experiments. **b, c:** Combined rate constants k_+k_n and k_+k_2, respectively. **d:** The individual rate constants calculated from k_+ and the combined constants. Figure adapted from **Paper V**

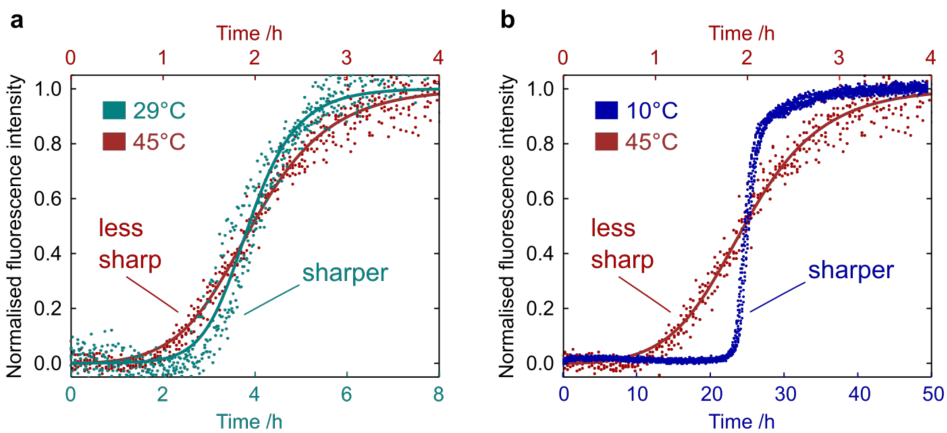

Figure 4.6: Comparison of the curve shapes at different temperatures. **(a)** between 29°C and 45°C. **(b)** between 10°C and 45°C.
Decreasing temperature gives sharper curves as the relative influence of secondary nucleation gets more prominent, compare figure 2.2C. Figure adapted from **Paper V**

Table 4.2: The derived free energy barriers and their enthalpic and entropic components for the different microscopic steps. Entropy term given at T = 298 K.

	Elongation	Primary nucleation	Secondary nucleation
$\Delta H^{\ddagger\Theta}$ (kJmol^{-1})	55±5	144±25	-11± 7
T $\Delta S^{\ddagger\Theta}$(kJmol^{-1})	49±5	79±26	-27±8
$\Delta G^{\ddagger\Theta}$ (kJmol^{-1})	5±1	65±2	16±2

In an effort to dissect the different effect of temperature on the composite steps of secondary nucleation SPR binding experiments were performed, revealing that the fractional surface coverage increased at lower temperatures. We have seen previously that the surface coverage of fibrils can work in an analogous way to the fractional site occupancy in enzyme kinetics. It then seems to be the case that the actual conversion steps in secondary nucleation can have a similar energetic profile to those in primary nucleation and the main driver behind the increased relative prominence of secondary nucleation is the favouring of the fibril-associated state in colder solutions.

Chapter 5

Outlook

"And still I am there falling, down in this evil pit
But until I hit the bottom, I won't believe it's bottomless"
The Handsome Family: The Bottomless Hole

The aggregation pathway of amyloids and their role in disease has proven to be immensely complex. The literature on the subject can often seem labyrinthine, vast, and at many points rife with conflicting evidence. However, through a massive effort of thousands of researchers we are moving forward. For example, when it comes to the role of secondary nucleation, the image has gradually been growing more clear. In **Paper III**, in 2018, we formulated a number of questions pertaining to secondary nucleation. Even in the relatively short time that has passed since then, in some cases we are closer to an answer, and in some cases the questions themselves have become better defined. In this final chapter I will go through the questions again and discuss them in the light of new evidence, some of which is presented in the earlier chapters of this book.

1 Does secondary nucleation happen along the fibril sides?

The involvement of the fibril sides in secondary nucleation is at this point well supported. In **Paper III** we mentioned evidence based on secondary nucleation being selectively suppressed by molecules that bind to the fibril surface, such as Brichos [85] and antibodies [103, 104]. We also discussed evidence based on microscopy [66, 105], including the microscopy images in **Paper II**. In addition to this, it is a recurring theme throughout several studies that the effective rate of secondary nucleation scales

with the degree of surface coverage of fibrils. It seems like, no matter the nature of the following catalytic steps, attachment to the fibril surface is crucial in setting the pace for secondary nucleation. This also means that preventing surface attachment remains a valid approach to break the aggregation feedback loop and reduce the generation of oligomers.

2 Does secondary nucleation occur at defined sites or is it a diffuse process?

The precise nature of the catalytic sites along the fibril sides is more difficult to determine and remains an open question. The short structural repetition distance along fibril structures, the separation between two beta strands, would speak for overlapping sites or more diffuse character. On the other hand, it is also plausible that structural defects along newly formed fibrils serve as catalytic sites, in which case they would be more distinct in nature. Structural studies of the interaction between fibrils and attached species are challenging due to the heterogeneous and transient nature of such samples, but the findings in **Paper II** provide a promising starting point for future studies.

3 Does secondary nucleation involve the highly ordered fibril core structure or the flexible termini that decorate the fibril?

Recent work on variations in the amino acid composition and sequence in the N-terminal part of $A\beta$ [106] as well as on variations in charge in the same region [87] has shown that the N-terminus does indeed act as a modulator both of the rate and specificity of secondary nucleation. This is partly backed up by our findings in **Paper II**, that surface coverage of wt $A\beta 42$ is diminished on N-terminally truncated fibrils. However, the lack of cross nucleation between $A\beta 40$ and $A\beta 42$ [86], which have an identical N-terminal, suggests that the core region is also critical. In addition, recent work on mutations on exposed residues in the fibril core region has revealed that this too can act as a determinant of specificity by way of modulating the core structure [107]. It would seem like control over secondary nucleation is not a feature that is exclusive to one specific part of the protein.

4 Do oligomers form in solution or at the fibrils surface?

There is no doubt, of course, that prefibrillar oligomers can form spontaneously in solution. The question is whether such oligomerization necessarily precedes attachment to the fibril surface. In **Paper III**, we referred to a simulation made in a minimal system wherein Lennard-Jones particles at an intermediate level of supersaturation tended to form unstructured oligomers that would , on contact with a crystal surface, take up the structure of that crystal [108]. The net effect of such a mechanism would be to reduce the number of oligomers in solution. In amyloid aggregation the reverse seems to be the case, making it more likely that the net flow of the reaction is attachment of monomers and release of oligomers.

5 Does structural conversion happen before or after detachment?

The circumstances of structural conversion is a crucial question as it relates to the nature of the species that are released from the fibrils, yet this remains a difficult question. Investigations into the time evolution of oligomer populations have shown a profile that suggests that fibrils can release of oligomers that have not yet undergone structural conversion into an elongation-competent form [109]. However, these released species are not in themselves a product of secondary nucleation. As mentioned at the end of chapter 2, the secondary nucleation rate constant reports on the net production of fully converted species, a process which may contain several steps. If the release of unstructured oligomers represent one of these steps, or happens in parallel to secondary nucleation, remains to be determined.

However, it is not clear whether the released oligomers undergo structural conversion in solution, subsequent to release, or structural conversion takes place on the fibril surface in parallel to the release of unstructured oligomers. The main challenge in settling this question is that once structural conversion has taken place the resulting species will rapidly elongate and become indistinguishable from other fibrils.

6 What is the driving force for detachment?

Since amyloid fibrils characteristically do not branch it is clear that secondary nucleation involves detachment from the parent fibril. In addition, elevated oligomer populations would not be detected were it not for efficient detachment. Efficient catalysis requires an intermediate affinity between the substrate/product and the cata-

lytic surface strong enough to promote binding, but not so strong as to impair release [73]. **Paper V** shed some light on the energetics of secondary nucleation, revealing that the net free energy barrier for secondary nucleation is entropic in nature, with a favourable enthalpic term. However, it was further seen that this profile is determined by the attachment to the fibril surface, the subsequent steps have a thermodynamic signature that is similar to that of primary nucleation, suggesting that the driving forces could be similar. It has been speculated that shear forces might enhance the rate of secondary nucleation by speeding up the release, but in the case of amyloid formation this remains to be tested .

7 Is secondary nucleation the origin of strain propagation?

Connected to the nature and circumstances of structural conversion is the question of whether the products of secondary nucleation take up the fold structure of the parent fibril. It seems plausible that structural conversion on the fibril surface would indeed propagate structure, but if the conversion happens in solution this is more difficult to imagine. Experiments have shown that when cross-reacting $A\beta 40$ and $A\beta 42$, parent fibril structure is propagated through elongation, but not through secondary nucleation [110]. Similarly, in work on α-synuclein, where different folds are favoured by different solution conditions, has shown that surface catalyzed aggregates do not take on the structure of a parent fibril made in a different condition [111].

8 What is the role of secondary nucleation in amyloid pathology and spreading?

This final question is the one that motivates all the others and it remains a challenge.We have seen that secondary nucleation can act as a major source of oligomers and that these can be toxic. We have also seen, in **Paper I**, that secondary nucleation remains active in human CSF. We have also seen, in papers **II** and **IV**, that the aggregation propensity of $A\beta$ can be enhance by altering solution conditions, providing a possible explanation of how aggregation may extend into the typically much lower peptide concentrations *in vivo*. In conclusion, exploring secondary nucleation remains a promising approach for uncovering the molecular mechanisms of pathological amyloid formation.

Bibliography

[1] R Brookmeyer, S Gray and C Kawas. 'Projections of Alzheimer's disease in the United States and the public health impact of delaying disease onset.' In: *American Journal of Public Health* 88.9 (Sept. 1998), pp. 1337–1342.

[2] H. Niu et al. 'Prevalence and incidence of Alzheimer's disease in Europe: A meta-analysis'. In: *Neurología (English Edition)* 32.8 (Oct. 2017), pp. 523–532.

[3] Ron Brookmeyer et al. 'Forecasting the prevalence of preclinical and clinical Alzheimer's disease in the United States'. In: *Alzheimer's & Dementia* 14.2 (Feb. 2018), pp. 121–129.

[4] Philip Scheltens et al. 'Alzheimer's disease'. In: *The Lancet* 388.10043 (July 2016), pp. 505–517.

[5] Jun-Young Lee et al. 'Illiteracy and the incidence of Alzheimer's disease in the Yonchon County survey, Korea'. In: *International Psychogeriatrics* 20.5 (Oct. 2008).

[6] Masoud Hoore et al. 'Mathematical model shows how sleep may affect amyloid fibrillization'. In: *bioRxiv* (1st Sept. 2019).

[7] Janine K. Cataldo, Judith J. Prochaska and Stanton A. Glantz. 'Cigarette Smoking is a Risk Factor for Alzheimer's Disease: An Analysis Controlling for Tobacco Industry Affiliation'. In: *Journal of Alzheimer's Disease* 19.2 (7th Jan. 2010), pp. 465–480.

[8] M. A. Beydoun, H. A. Beydoun and Y. Wang. 'Obesity and central obesity as risk factors for incident dementia and its subtypes: a systematic review and meta-analysis'. In: *Obesity Reviews* 9.3 (May 2008), pp. 204–218.

[9] Miia Kivipelto et al. 'Obesity and Vascular Risk Factors at Midlife and the Risk of Dementia and Alzheimer Disease'. In: *Archives of Neurology* 62.10 (1st Oct. 2005).

[10] Zoe Arvanitakis et al. 'Diabetes Mellitus and Risk of Alzheimer Disease and Decline in Cognitive Function'. In: *Archives of Neurology* 61.5 (1st May 2004), p. 661.

[11] Renée FAG de Bruijn et al. 'The potential for prevention of dementia across two decades: the prospective, population-based Rotterdam Study'. In: *BMC Medicine* 13.1 (Dec. 2015).

[12] C. Bancher et al. 'Accumulation of abnormally phosphorylated ⊠ precedes the formation of neurofibrillary tangles in Alzheimer's disease'. In: *Brain Research* 477.1 (Jan. 1989), pp. 90–99.

[13] G. G. Glenner and C. W. Wong. 'Alzheimer's disease: initial report of the purification and characterization of a novel cerebrovascular amyloid protein'. In: *Biochemical and Biophysical Research Communications* 120.3 (16th May 1984), pp. 885–890.

[14] C. L. Masters et al. 'Amyloid plaque core protein in Alzheimer disease and Down syndrome'. In: *Proceedings of the National Academy of Sciences of the United States of America* 82.12 (June 1985), pp. 4245–4249.

[15] Jie Kang et al. 'The precursor of Alzheimer's disease amyloid A4 protein resembles a cell-surface receptor'. In: *Nature* 325.6106 (Feb. 1987), pp. 733–736.

[16] Takeshi Iwatsubo et al. 'Visualization of Aβ42 (43) and Aβ40 in senile plaques with end-specific Aβ monoclonals: evidence that an initially deposited species is Aβ42 (43)'. In: *Neuron* 13.1 (1994). ISBN: 0896-6273 Publisher: Cell Press, pp. 45–53.

[17] Autumn M. Klein, Neil W. Kowall and Robert J. Ferrante. 'Neurotoxicity and Oxidative Damage of Beta Amyloid 1-42 versus Beta Amyloid 1-40 in the Mouse Cerebral Cortex'. In: *Annals of the New York Academy of Sciences* 893.1 (Nov. 1999), pp. 314–320.

[18] M. C. Chartier-Harlin et al. 'Early-onset Alzheimer's disease caused by mutations at codon 717 of the beta-amyloid precursor protein gene'. In: *Nature* 353.6347 (31st Oct. 1991), pp. 844–846.

[19] Alison Goate et al. 'Segregation of a missense mutation in the amyloid precursor protein gene with familial Alzheimer's disease'. In: *Nature* 349.6311 (Feb. 1991), pp. 704–706.

[20] M. Mullan et al. 'A pathogenic mutation for probable Alzheimer's disease in the APP gene at the N-terminus of beta-amyloid'. In: *Nature Genetics* 1.5 (Aug. 1992), pp. 345–347.

[21] J. A. Hardy and G. A. Higgins. 'Alzheimer's disease: the amyloid cascade hypothesis'. In: *Science (New York, N.Y.)* 256.5054 (10th Apr. 1992), pp. 184–185.

[22] John Hardy. 'Alzheimer's disease: The amyloid cascade hypothesis: An update and reappraisal'. In: *Journal of Alzheimer's Disease* 9 (s3 27th July 2006), pp. 151–153.

[23] M. P. Lambert et al. 'Diffusible, nonfibrillar ligands derived from $A\beta$1-42 are potent central nervous system neurotoxins'. In: *Proceedings of the National Academy of Sciences* 95.11 (26th May 1998), pp. 6448–6453.

[24] Hilal A. Lashuel and Peter T. Lansbury. 'Are amyloid diseases caused by protein aggregates that mimic bacterial pore-forming toxins?' In: *Quarterly Reviews of Biophysics* 39.2 (May 2006), pp. 167–201.

[25] Hilal A. Lashuel et al. 'Amyloid pores from pathogenic mutations'. In: *Nature* 418.6895 (July 2002), pp. 291–291.

[26] Byron Caughey and Peter T. Lansbury. 'Protofibrils, Pores, Fibrils, and Neurodegeneration: Separating the Responsible Protein Aggregates from The Innocent Bystanders'. In: *Annual Review of Neuroscience* 26.1 (Mar. 2003), pp. 267–298.

[27] G. Bitan et al. 'Amyloid -protein ($A\beta$) assembly: $A\beta$40 and $A\beta$42 oligomerize through distinct pathways'. In: *Proceedings of the National Academy of Sciences* 100.1 (7th Jan. 2003), pp. 330–335.

[28] Naoki Yamamoto et al. 'A Ganglioside-induced Toxic Soluble Aβ Assembly: ITS ENHANCED FORMATION FROM AβBEARING THE ARCTIC MUTATION'. In: *Journal of Biological Chemistry* 282.4 (26th Jan. 2007), pp. 2646–2655.

[29] Brett A. Chromy et al. 'Self-Assembly of Aβ $_{1-42}$ into Globular Neurotoxins †'. In: *Biochemistry* 42.44 (Nov. 2003), pp. 12749–12760.

[30] C Behl. 'Hydrogen peroxide mediates amyloid β protein toxicity'. In: *Cell* 77.6 (17th June 1994), pp. 817–827.

[31] C. Behl. 'Amyloid β-protein toxicity and oxidative stress in Alzheimer's disease'. In: *Cell and Tissue Research* 290.3 (26th Nov. 1997), pp. 471–480.

[32] J. N. Keller et al. 'Evidence of increased oxidative damage in subjects with mild cognitive impairment'. In: *Neurology* 64.7 (12th Apr. 2005), pp. 1152–1156.

[33] M. Rapoport et al. 'Tau is essential to -amyloid-induced neurotoxicity'. In: *Proceedings of the National Academy of Sciences* 99.9 (30th Apr. 2002), pp. 6364–6369.

[34] Salvatore Oddo et al. 'Aβ Immunotherapy Leads to Clearance of Early, but Not Late, Hyperphosphorylated Tau Aggregates via the Proteasome'. In: *Neuron* 43.3 (Aug. 2004), pp. 321–332.

[35] Khalid Iqbal et al. 'Tau pathology in Alzheimer disease and other tauopathies'. In: *Biochimica et Biophysica Acta (BBA) - Molecular Basis of Disease* 1739.2 (Jan. 2005), pp. 198–210.

[36] E. D. Roberson et al. 'Reducing Endogenous Tau Ameliorates Amyloid -Induced Deficits in an Alzheimer's Disease Mouse Model'. In: *Science* 316.5825 (4th May 2007), pp. 750–754.

[37] Christopher J. Dunning et al. 'Direct High Affinity Interaction between Aβ42 and GSK3α Stimulates Hyperphosphorylation of Tau. A New Molecular Link in Alzheimer's Disease?' In: *ACS Chemical Neuroscience* 7.2 (17th Feb. 2016), pp. 161–170.

[38] D. A. Kirschner, C. Abraham and D. J. Selkoe. 'X-ray diffraction from intraneuronal paired helical filaments and extraneuronal amyloid fibers in Alzheimer disease indicates cross-beta conformation.' In: *Proceedings of the National Academy of Sciences* 83.2 (1st Jan. 1986), pp. 503–507.

[39] Marielle Aulikki Wälti et al. 'Atomic-resolution structure of a disease-relevant Aβ(1–42) amyloid fibril'. In: *Proceedings of the National Academy of Sciences* 113.34 (23rd Aug. 2016), E4976–E4984.

[40] Michael T. Colvin et al. 'Atomic Resolution Structure of Monomorphic Aβ $_{42}$ Amyloid Fibrils'. In: *Journal of the American Chemical Society* 138.30 (3rd Aug. 2016), pp. 9663–9674.

[41] A. K. Paravastu et al. 'Molecular structural basis for polymorphism in Alzheimer's -amyloid fibrils'. In: *Proceedings of the National Academy of Sciences* 105.47 (25th Nov. 2008), pp. 18349–18354.

[42] A. T. Petkova et al. 'A structural model for Alzheimer's -amyloid fibrils based on experimental constraints from solid state NMR'. In: *Proceedings of the National Academy of Sciences* 99.26 (24th Dec. 2002), pp. 16742–16747.

[43] Aneta T. Petkova, Wai-Ming Yau and Robert Tycko. 'Experimental Constraints on Quaternary Structure in Alzheimer's β-Amyloid Fibrils †'. In: *Biochemistry* 45.2 (Jan. 2006), pp. 498–512.

[44] Ivano Bertini et al. 'A New Structural Model of Aβ $_{40}$ Fibrils'. In: *Journal of the American Chemical Society* 133.40 (12th Oct. 2011), pp. 16013–16022.

[45] Lisa R. Volpatti et al. 'A Clear View of Polymorphism, Twist, and Chirality in Amyloid Fibril Formation'. In: *ACS Nano* 7.12 (23rd Dec. 2013), pp. 10443–10448.

[46] Jessica Meinhardt et al. 'Aβ(1-40) Fibril Polymorphism Implies Diverse Interaction Patterns in Amyloid Fibrils'. In: *Journal of Molecular Biology* 386.3 (Feb. 2009), pp. 869–877.

[47] Marcus Fändrich, Jessica Meinhardt and Nikolaus Grigorieff. 'Structural polymorphism of Alzheimer Aβ and other amyloid fibrils'. In: *Prion* 3.2 (Apr. 2009), pp. 89–93.

[48] Liisa Lutter et al. 'The molecular lifecycle of amyloid – Mechanism of assembly, mesoscopic organisation, polymorphism, suprastructures, and biological consequences'. In: *Biochimica et Biophysica Acta (BBA) - Proteins and Proteomics* 1867.11 (Nov. 2019), p. 140257.

[49] W Klein. 'Targeting small Aβ oligomers: the solution to an Alzheimer's disease conundrum?' In: *Trends in Neurosciences* 24.4 (1st Apr. 2001), pp. 219–224.

[50] Dominic M. Walsh et al. 'Naturally secreted oligomers of amyloid beta protein potently inhibit hippocampal long-term potentiation in vivo'. In: *Nature* 416.6880 (4th Apr. 2002), pp. 535–539.

[51] Sandra Chimon et al. 'Evidence of fibril-like β-sheet structures in a neurotoxic amyloid intermediate of Alzheimer's β-amyloid'. In: *Nature Structural & Molecular Biology* 14.12 (Dec. 2007), pp. 1157–1164.

[52] Dean M. Hartley et al. 'Protofibrillar Intermediates of Amyloid β-Protein Induce Acute Electrophysiological Changes and Progressive Neurotoxicity in Cortical Neurons'. In: *The Journal of Neuroscience* 19.20 (15th Oct. 1999), pp. 8876–8884.

[53] Annalisa Relini et al. 'Detection of Populations of Amyloid-Like Protofibrils with Different Physical Properties'. In: *Biophysical Journal* 98.7 (Apr. 2010), pp. 1277–1284.

[54] Mahiuddin Ahmed et al. 'Structural conversion of neurotoxic amyloid-β1–42 oligomers to fibrils'. In: *Nature Structural & Molecular Biology* 17.5 (May 2010), pp. 561–567.

[55] Bertrand Morel et al. 'Dynamic micellar oligomers of amyloid beta peptides play a crucial role in their aggregation mechanisms'. In: *Physical Chemistry Chemical Physics* 20.31 (2018), pp. 20597–20614.

[56] Sudhakar Parthasarathy et al. 'Structural Insight into an Alzheimer's Brain-Derived Spherical Assembly of Amyloid β by Solid-State NMR'. In: *Journal of the American Chemical Society* 137.20 (27th May 2015), pp. 6480–6483.

[57] Mimi Nick et al. 'A long-lived Aβ oligomer resistant to fibrillization'. In: *Biopolymers* (10th Jan. 2018), e23096.

[58] Dominic M. Walsh et al. 'A facile method for expression and purification of the Alzheimer's disease-associated amyloid β-peptide: Expression and purification of the amyloid β-peptide'. In: *FEBS Journal* 276.5 (Mar. 2009), pp. 1266–1281.

[59] Erik Hellstrand et al. 'Amyloid β-Protein Aggregation Produces Highly Reproducible Kinetic Data and Occurs by a Two-Phase Process'. In: *ACS Chemical Neuroscience* 1.1 (20th Jan. 2010), pp. 13–18.

[60] S. I. A. Cohen et al. 'Proliferation of amyloid-β42 aggregates occurs through a secondary nucleation mechanism'. In: *Proceedings of the National Academy of Sciences* 110.24 (11th June 2013), pp. 9758–9763.

[61] Georg Meisl et al. 'Molecular mechanisms of protein aggregation from global fitting of kinetic models'. In: *Nature Protocols* 11.2 (Feb. 2016), pp. 252–272.

[62] Alexander J. Dear et al. 'The catalytic nature of protein aggregation'. In: *The Journal of Chemical Physics* 152.4 (31st Jan. 2020), p. 045101.

[63] Frank A. Ferrone, James Hofrichter and William A. Eaton. 'Kinetics of sickle hemoglobin polymerization'. In: *Journal of Molecular Biology* 183.4 (June 1985), pp. 611–631.

[64] S. G. Agrawal and A. H. J. Paterson. 'Secondary Nucleation: Mechanisms and Models'. In: *Chemical Engineering Communications* 202.5 (4th May 2015), pp. 698–706.

[65] Georg Meisl et al. 'Differences in nucleation behavior underlie the contrasting aggregation kinetics of the Aβ40 and Aβ42 peptides'. In: *Proceedings of the National Academy of Sciences* 111.26 (1st July 2014), pp. 9384–9389.

[66] Ricardo Gaspar et al. 'Secondary nucleation of monomers on fibril surface dominates α-synuclein aggregation and provides autocatalytic amyloid amplification'. In: *Quarterly Reviews of Biophysics* 50 (2017).

[67] A. M. Ruschak and A. D. Miranker. 'Fiber-dependent amyloid formation as catalysis of an existing reaction pathway'. In: *Proceedings of the National Academy of Sciences* 104.30 (24th July 2007), pp. 12341–12346.

[68] Vito Foderà et al. 'Secondary Nucleation and Accessible Surface in Insulin Amyloid Fibril Formation'. In: *The Journal of Physical Chemistry B* 112.12 (Mar. 2008), pp. 3853–3858.

[69] Casper B. Rasmussen et al. 'Imperfect repeats in the functional amyloid protein FapC reduce the tendency to fragment during fibrillation: Imperfect Repeats in Functional Amyloid'. In: *Protein Science* 28.3 (Mar. 2019), pp. 633–642.

[70] Samuel I. A. Cohen et al. 'Nucleated polymerization with secondary pathways. II. Determination of self-consistent solutions to growth processes described by non-linear master equations'. In: *The Journal of Chemical Physics* 135.6 (14th Aug. 2011), p. 065106.

[71] Georg Meisl et al. 'Quantitative analysis of intrinsic and extrinsic factors in the aggregation mechanism of Alzheimer-associated Aβ-peptide'. In: *Scientific Reports* 6.1 (May 2016).

[72] Georg Meisl et al. 'A general reaction network unifies the aggregation behaviour of the Aβ42 peptide and its variants'. In: *arXiv:1604.00828 [q-bio]* (4th Apr. 2016). arXiv: 1604.00828.

[73] Anđela Šarić et al. 'Physical determinants of the self-replication of protein fibrils'. In: *Nature Physics* 12.9 (18th July 2016), pp. 874–880.

[74] Leonor Menten and MI Michaelis. 'Die kinetik der invertinwirkung'. In: *Biochem Z* 49.333-369 (1913), p. 5.

[75] William P. Esler et al. 'Alzheimer's Disease Amyloid Propagation by a Template-Dependent Dock-Lock Mechanism †'. In: *Biochemistry* 39.21 (May 2000), pp. 6288–6295.

[76] T. Scheibel, J. Bloom and S. L. Lindquist. 'The elongation of yeast prion fibers involves separable steps of association and conversion'. In: *Proceedings of the National Academy of Sciences* 101.8 (24th Feb. 2004), pp. 2287–2292.

[77] Eri Chatani et al. 'Pre-Steady-State Kinetic Analysis of the Elongation of Amyloid Fibrils of β2-Microglobulin with Tryptophan Mutagenesis'. In: *Journal of Molecular Biology* 400.5 (July 2010), pp. 1057–1066.

[78] Marco Bacci et al. 'Amyloid β Fibril Elongation by Monomers Involves Disorder at the Tip'. In: *Journal of Chemical Theory and Computation* 13.10 (10th Oct. 2017), pp. 5117–5130.

[79] Ph Sa Vassar and CF Culling. 'Fluorescent stains, with special reference to amyloid and connective tissues.' In: *Archives of pathology* 68 (1959), pp. 487–498.

[80] Hironobu Naiki et al. 'Fluorometric determination of amyloid fibrils in vitro using the fluorescent dye, thioflavine T'. In: *Analytical Biochemistry* 177.2 (Mar. 1989), pp. 244–249.

[81] Eduardo Coelho-Cerqueira, Anderson S. Pinheiro and Cristian Follmer. 'Pitfalls associated with the use of Thioflavin-T to monitor anti-fibrillogenic activity'. In: *Bioorganic & Medicinal Chemistry Letters* 24.14 (July 2014), pp. 3194–3198.

[82] David J. Lindberg et al. 'Binding of Thioflavin-T to Amyloid Fibrils Leads to Fluorescence Self-Quenching and Fibril Compaction'. In: *Biochemistry* 56.16 (25th Apr. 2017), pp. 2170–2174.

[83] Kirsten Gade Malmos et al. 'ThT 101: a primer on the use of thioflavin T to investigate amyloid formation'. In: *Amyloid* 24.1 (2nd Jan. 2017), pp. 1–16.

[84] Adrian M. Isaacs et al. 'Acceleration of Amyloid β-Peptide Aggregation by Physiological Concentrations of Calcium'. In: *Journal of Biological Chemistry* 281.38 (22nd Sept. 2006), pp. 27916–27923.

[85] Samuel I A Cohen et al. 'A molecular chaperone breaks the catalytic cycle that generates toxic Aβ oligomers'. In: *Nature Structural & Molecular Biology* 22.3 (Mar. 2015), pp. 207–213.

[86] Risto Cukalevski et al. 'The Aβ40 and Aβ42 peptides self-assemble into separate homomolecular fibrils in binary mixtures but cross-react during primary nucleation'. In: *Chem. Sci.* 6.7 (2015), pp. 4215–4233.

[87] Kalyani Sanagavarapu et al. 'N-terminal sequence determinants of secondary nucleation'. In: *In preparation* ().

[88] Therése Klingstedt et al. 'Synthesis of a library of oligothiophenes and their utilization as fluorescent ligands for spectral assignment of protein aggregates'. In: *Organic & Biomolecular Chemistry* 9.24 (2011), p. 8356.

[89] Katarzyna M. Psonka-Antonczyk et al. 'Nanoscale Structure and Spectroscopic Probing of Aβ1-40 Fibril Bundle Formation'. In: *Frontiers in Chemistry* 4 (22nd Nov. 2016).

[90] Sofie Nyström et al. 'Imaging Amyloid Tissues Stained with Luminescent Conjugated Oligothiophenes by Hyperspectral Confocal Microscopy and Fluorescence Lifetime Imaging'. In: *Journal of Visualized Experiments* 128 (20th Oct. 2017).

[91] Lauren S. Whyte et al. 'Endo-lysosomal and autophagic dysfunction: a driving factor in Alzheimer's disease?' In: *Journal of Neurochemistry* 140.5 (Mar. 2017), pp. 703–717.

[92] E.H. Koo et al. 'Trafficking of cell-surface amyloid beta-protein precursor. I. Secretion, endocytosis and recycling as detected by labeled monoclonal antibody'. In: *Journal of Cell Science* 109.5 (1st May 1996), p. 991.

[93] Anne M. Cataldo et al. 'Aβ localization in abnormal endosomes: association with earliest Aβ elevations in AD and Down syndrome'. In: *Neurobiology of Aging* 25.10 (Nov. 2004), pp. 1263–1272.

[94] Rui-Qin Liu et al. 'Membrane Localization of β-Amyloid 1–42 in Lysosomes: A POSSIBLE MECHANISM FOR LYSOSOME LABILIZATION'. In: *Journal of Biological Chemistry* 285.26 (25th June 2010), pp. 19986–19996.

[95] Paul M. Gorman et al. 'Alternate Aggregation Pathways of the Alzheimer β-Amyloid Peptide: Aβ Association Kinetics at Endosomal pH'. In: *Journal of Molecular Biology* 325.4 (Jan. 2003), pp. 743–757.

[96] Ann-Sofi Johansson et al. 'Physiochemical characterization of the Alzheimer's disease-related peptides *Aβ*1-42Arctic and *Aβ*1-42wt'. In: *FEBS Journal* 273.12 (June 2006), pp. 2618–2630.

[97] J. Khandogin and C. L. Brooks. 'Linking folding with aggregation in Alzheimer's beta-amyloid peptides'. In: *Proceedings of the National Academy of Sciences* 104.43 (23rd Oct. 2007), pp. 16880–16885.

[98] Joseph A. Kotarek, Kathryn C. Johnson and Melissa A. Moss. 'Quartz crystal microbalance analysis of growth kinetics for aggregation intermediates of the amyloid-β protein'. In: *Analytical Biochemistry* 378.1 (July 2008), pp. 15–24.

[99] Kristoffer Brännström et al. 'The N-terminal Region of Amyloid β Controls the Aggregation Rate and Fibril Stability at Low pH Through a Gain of Function Mechanism'. In: *Journal of the American Chemical Society* 136.31 (6th Aug. 2014), pp. 10956–10964.

[100] Kristoffer Brännström et al. 'The role of histidines in amyloid β fibril assembly'. In: *FEBS Letters* 591.8 (Apr. 2017), pp. 1167–1175.

[101] Yeu Su and Pei-Teh Chang. 'Acidic pH promotes the formation of toxic fibrils from β-amyloid peptide'. In: *Brain Research* 893.1 (Mar. 2001), pp. 287–291.

[102] Karolina L. Zapadka et al. 'A pH-Induced Switch in Human Glucagon-like Peptide-1 Aggregation Kinetics'. In: *Journal of the American Chemical Society* 138.50 (21st Dec. 2016), pp. 16259–16265.

[103] Francesco A. Aprile et al. 'Selective targeting of primary and secondary nucleation pathways in Aβ42 aggregation using a rational antibody scanning method'. In: *Science Advances* 3.6 (June 2017), e1700488.

[104] Anna Munke et al. 'Phage display and kinetic selection of antibodies that specifically inhibit amyloid self-replication'. In: *Proceedings of the National Academy of Sciences* 114.25 (20th June 2017), pp. 6444–6449.

[105] Jae Sun Jeong et al. 'Novel Mechanistic Insight into the Molecular Basis of Amyloid Polymorphism and Secondary Nucleation during Amyloid Formation'. In: *Journal of Molecular Biology* 425.10 (May 2013), pp. 1765–1781.

[106] Kalyani Sanagavarapu et al. 'Specific sequence of the flexible N-terminal tail plays a key role in the secondary nucleation of $A\beta 42$'. In: *In preparation* ().

[107] Dev Thacker et al. 'The role of fibril structure and surface hydrophobicity in secondary nucleation of amyloid fibrils'. In: *PNAS, in preparation* ().

[108] Jamshed Anwar, Shahzeb Khan and Lennart Lindfors. 'Secondary Crystal Nucleation: Nuclei Breeding Factory Uncovered'. In: *Angewandte Chemie* 127.49 (1st Dec. 2015), pp. 14894–14897.

[109] Thomas C. T. Michaels et al. 'Dynamics of oligomer populations formed during the aggregation of Alzheimer's Aβ42 peptide'. In: *Nature Chemistry* (13th Apr. 2020).

[110] Kristoffer Brännström et al. 'The Properties of Amyloid-β Fibrils Are Determined by their Path of Formation'. In: *Journal of Molecular Biology* 430.13 (June 2018), pp. 1940–1949.

[111] Alessia Peduzzo, Sara Linse and Alexander K. Buell. 'The Properties of α-Synuclein Secondary Nuclei Are Dominated by the Solution Conditions Rather than the Seed Fibril Strain'. In: *ACS Chemical Neuroscience* 11.6 (18th Mar. 2020), pp. 909–918.

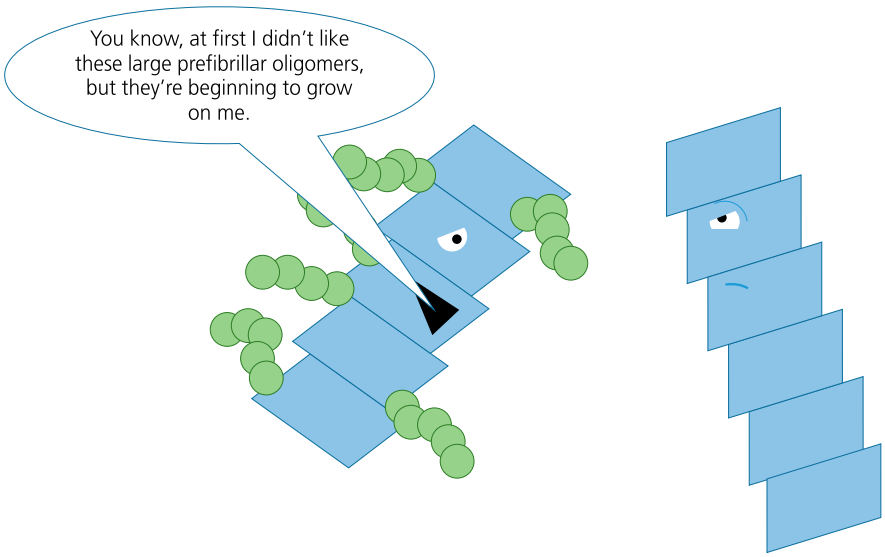

Printed by Media-Tryck, Lund 2020 NORDIC SWAN ECOLABEL 3041 0903

LUND UNIVERSITY

ISBN: 978-91-7422-740-6

Biochemistry and Structural Biology
Faculty of Science
Lund University

Secondary nucleation in amyloid aggregation

MATTIAS TÖRNQUIST | BIOCHEMISTRY AND STRUCTURAL BIOLOGY | LUND UNIVERSITY

$$\frac{dP}{dT} = k_n \frac{m(t)^{n_c}}{1 + \left(\frac{m(t)}{K_P}\right)^{n_c}} + k_2 \frac{m(t)^{n_2}}{1 + \left(\frac{m(t)}{K_S}\right)^{n_2}} M(t)$$

$$\frac{dM}{dT} = 2k_+ \frac{m(t)}{1 + \frac{m(t)}{K_E}} P(t)$$